NBER WORKING PAPER SERIES

IMPROVED TRANSPORTATION NETWORKS FACILITATE ADAPTATION TO POLLUTION AND TEMPERATURE EXTREMES

Panle Jia Barwick
Dave Donaldson
Shanjun Li
Yatang Lin
Deyu Rao

Working Paper 30462
http://www.nber.org/papers/w30462

NATIONAL BUREAU OF ECONOMIC RESEARCH
1050 Massachusetts Avenue
Cambridge, MA 02138
September 2022

We thank Nahim Bin Zahur and Ziye Zhang for excellent research assistance, and Minwei Tang for data support. The views expressed herein are those of the authors and do not necessarily reflect the views of the National Bureau of Economic Research.

NBER working papers are circulated for discussion and comment purposes. They have not been peer-reviewed or been subject to the review by the NBER Board of Directors that accompanies official NBER publications.

© 2022 by Panle Jia Barwick, Dave Donaldson, Shanjun Li, Yatang Lin, and Deyu Rao. All rights reserved. Short sections of text, not to exceed two paragraphs, may be quoted without explicit permission provided that full credit, including © notice, is given to the source.

Improved Transportation Networks Facilitate Adaptation to Pollution and Temperature Extremes
Panle Jia Barwick, Dave Donaldson, Shanjun Li, Yatang Lin, and Deyu Rao
NBER Working Paper No. 30462
September 2022
JEL No. O18,Q53,Q54,R41

ABSTRACT

The social costs of pollution and climate change hinge critically on humans' ability to adapt. Based on transaction records from the world's largest payment network, this research compiles daily travel flows and documents that China's rapid expansion of high-speed railways (HSR) facilitates the use of intercity travel as an effective adaptation strategy. Access to HSR reduces travelers' exposure to extreme air pollution and temperature by 7% and 10%, leading to substantial health benefits. These reductions are attributed to both contemporaneous responses to unexpected adverse conditions and also longer-horizon changes in travel patterns.

Panle Jia Barwick
University of Wisconsin-Madison
Department of Economics
1180 Observatory Dr
Madison, WI 53706
and NBER
panle.barwick@gmail.com

Dave Donaldson
Department of Economics, E52-554
MIT
77 Massachusetts Avenue
Cambridge, MA 02139
and NBER
ddonald@mit.edu

Shanjun Li
Cornell University
405 Warren Hall
Ithaca, NY 14853
and NBER
SL2448@cornell.edu

Yatang Lin
Department of Economics
Hong Kong University of Science
and Technology
Hong Kong
yatang.lin@gmail.com

Deyu Rao
Department of Economics
Hong Kong University of Science
and Technology
Hong Kong
dyrao@ust.hk

1 Introduction

Environmental degradation and climate change pose growing risks to humans.[1] The social costs of pollution and climate change depend crucially on the extent to which humans can adapt to extreme environmental conditions. While long-term migration could be an effective strategy to adapt to a changing environment (Banzhaf and Walsh, 2008; Deschênes and Moretti, 2009; Kahn, 2010; Freeman et al., 2019; Desmet et al., 2021), it entails significant costs especially for residents in developing countries with severe market frictions and institutional constraints. In contrast, short-term intercity travel may offer a more practical and affordable adaptation strategy to reduce the negative effects of local environmental conditions. Indeed, "haze-avoidance tourism" and "smog refugees" have become important trends in intercity travel in China with the advent of cheap and fast transportation modes (Arlt, 2017; Sharkov, 2016; Chen et al., 2021).

This study provides to our knowledge the first analysis of how improved transportation infrastructure facilitates behavioral changes in response to adverse environmental conditions. Our analysis uses a unique data set of daily travel flows between all city-pairs in China, constructed based on credit and debit card transactions from the world's largest inter-bank payment network (UnionPay). The estimation takes advantage of the unprecedented and staggered expansion of high-speed railways (HSR) in China shown in Figure A1. Since 2008, China has built by far the largest HSR network in the world, reaching nearly 38,000 km by 2020 and more than twice as long as the HSR network of all other countries combined. In the meantime, with rapid economic growth and heavy reliance on fossil fuels, air pollution has become one of the most pressing challenges in large urban centers in China (Greenstone et al., 2021; The Health Effects Institute, 2019). Many Chinese cities regularly rank among the most polluted cities in the world. In addition, climate change has increased both the frequency and the intensity of heat waves, exacerbated by the heat island effect in mega cities (Ye et al., 2014; Luo and Lau, 2017). Pollution and temperature extremes raise serious concerns, given the size of the affected population in China and technological or financial constraints for adaptation, especially for the urban poor.

Our analysis uses an empirical framework that combines the difference-in-differences and triple-difference strategies: comparing the exposure to extreme air pollution and temperature among travelers from cities with HSR access to that among travelers from cities without such access, under different environmental conditions in home cities. The causal effect of HSR connection on adaptation to environmental extremes is quantified by the variation in travel patterns in response to envi-

[1] A large literature has documented various impacts of pollution and climate change on economic growth (Nordhaus, 2006; Dell et al., 2012; Carleton and Hsiang, 2016), social stability (Burke et al., 2010; Hsiang et al., 2013), and health (Deschênes et al., 2009; Currie and Neidell, 2005; Chen et al., 2013; Landrigan et al., 2018) among others.

ronmental conditions. The key identification assumption is that the timing of a city's connection to HSR network is not driven by or in response to unobserved factors that affect daily variation in travel patterns, after controlling for a rich set of fixed effects including city fixed effects, day-of-sample fixed effects. This is plausible as the exact connection date is often determined by idiosyncratic engineering and institutional factors. The event study analysis shows no clear trend in the outcome variable before the HSR connection, supporting our identification assumption.

Our results show that China's rapid expansion of its HSR network has facilitated the adaption to environmental extremes: residents can more easily travel to destinations that have better environmental conditions. When home cities are subject to pollution extremes, travelers from cities without HSR access are 12.8% more likely to experience these detrimental conditions than those from cities with HSR connection. When home cities encounter temperature extremes, travelers without HSR access are 27.7% more likely to expose to temperature extremes than those with HSR access. In comparison, when home cities are not subject to pollution or temperature extremes, travelers' exposure to environmental extremes is similar regardless of the HSR access. In terms of the underlying channels, longer travel distances as a result of the HSR expansion explain 43% of the reduction in exposure to extreme pollution and 50% of the reduction in exposure to extreme temperatures. The remaining effect can be attributed to travelers' ability to leverage HSR connection and deliberately choose destination cities with better environmental conditions, conditioning on the distance to the origin city. Longer term adaptation in travel patterns (including changes in travel distance) to predictable environmental conditions post the HSR access explains 71% of the reduction in extreme pollution exposure and 83% of the reduction in extreme temperature exposure. The remaining impacts are attributed to contemporaneous responses to environmental extremes. Altogether, these reductions in exposure to environmental extremes entail substantial health benefits through reduced mortality.

This study contributes to two strands of literature. First, a large literature examines the benefit of transportation networks through promoting the mobility of people and goods (Behrens and Pels, 2012; Donaldson, 2018; Bernard et al., 2019), fostering market integration (Baum-Snow, 2010; Zheng and Kahn, 2013; Faber, 2014; Donaldson and Hornbeck, 2016; Lin, 2017), and facilitating knowledge sharing (Agrawal et al., 2017; Dong et al., 2020). Leveraging the rapid expansion of the HSR network in China and high-frequency data on intercity travel, our paper adds to this literature by demonstrating how improved transportation networks can facilitate adaptation to air pollution and temperature extremes. Second, this paper contributes to the literature on adaptation to adverse environmental conditions such as climate change and local pollution. Studies show that behavioral changes play an important role in mitigating the risks associated with air pollution and

climate change through reducing outdoor activities (Graff Zivin and Neidell, 2014; Moretti and Neidell, 2011a; Barwick et al., 2020), increasing defensive investments (Barreca et al., 2016; Ito and Zhang, 2020; Zheng and Kahn, 2017; Zhang and Mu, 2018), as well as changing residential locations (Banzhaf and Walsh, 2008; Bayer et al., 2009; Deschênes and Moretti, 2009; Kahn, 2010; Black et al., 2011; Chen et al., 2017; Freeman et al., 2019; Balboni, 2021; Cruz and Rossi-Hansberg, 2021). Our study demonstrates that improved transportation infrastructure renders short-term intercity travel another important adaptation strategy to mitigate the negative effects of adverse environmental conditions.

2 Data and Descriptive Evidence

Intercity Travel Flow We construct daily bilateral passenger flows across cities by leveraging the universe of credit and debit card transactions conducted through the UnionPay network. UnionPay is the only inter-bank payment network in China, and the largest network in the world. The database covers 34 trillion *yuan* ($4.9 trillion) of annual economic activities from 2.7 billion cards from 2011 to 2016. The date and location information of transaction records allows us to trace traveler flows between city pairs on a daily basis. This enables us to overcome a major data limitation in the literature where high-frequency measures of city-pair travel flows at the national level are unavailable until very recently with the proliferation of mobile positioning data.

Our traveler flow is calculated from a 1% card sample, which includes the stream of transactions made by 270 million cards during 2013-2016. We focus on offline transactions, for which the cardholder is physically present at the merchant's location. A trip occurs if the city of the transaction differs from the home city.[2] Using credit and debit cards is a popular payment method and accounted for over 40% of national retail consumption during our data period. Electronic payment methods such as Wechat and Alipay were limited during our data period, accounting for less than 2% of aggregate retail sales in 2013 and about 10% in 2016.

To examine the quality of our intercity travel flows based on card transactions data, we compare our data on travel flows with intercity mobility data from Baidu Migration by Baidu Maps, China's leading provider of digital map and online navigation services. Baidu migration data report population inflows from the top 100 origin cities and outflows to the top 100 destination cities between January 21 and March 23 in 2019 and between January 10 and March 15 in 2020.[3] The data are based on the location of over 600 million users of Baidu's location-based services, hence providing

[2]We limit our sample to trips up to seven days. The majority of trips last for one to two days.

[3]Source: http://qianxi.baidu.com/. Baidu Migration data aim to help understand population flows during the Chinese New Year so the data duration centers around the time of Chinese New Year. The data are only available from 2019.

good coverage and accuracy. Panels (a) and (b) in Appendix Figure A2 show that the two measures of intercity travels have high correlations, with a R^2 of 0.79 for both outflows and inflows. Panel (c) depicts the coefficient estimates of a gravity equation where the travel frequencies between city pairs (in logarithm) from the two data sources are separately regressed on flexible distance bins between the origin and destination cities. The coefficient estimates based on the UnionPay and Baidu data are very close to each other across all distance bins. These validation exercises confirm the high quality of our travel flow measures based on card transactions data.

Air Pollution and Temperature Data Air quality data come from China's Ministry of Ecology and Environment (MEE, formerly the Ministry of Environmental Protection). From 2013, ground-level monitoring stations were installed or upgraded in over 1600 sites throughout China and hourly air quality data from these monitoring stations are publicly reported on the MEE website. The number of monitoring stations and cities covered increased steadily from 1003 stations in 159 cities in 2013 to 1615 stations in 367 cities in 2015. We calculate the daily concentration of $PM_{2.5}$ at the city-daily level by averaging hourly readings from monitoring stations within a city. The nationwide average concentration of $PM_{2.5}$ during the 2013-2016 period was 48 $\mu g/m^3$ (with a standard deviation of 41 $\mu g/m^3$), much higher than the annual air quality standards of 12 $\mu g/m^3$ set by the U.S. Environmental Protection Agency and 35 $\mu g/m^3$ by China's MEE.

We collect hourly temperature data from NOAA's Integrated Surface Database (ISD) for all weather stations in China. ISD includes 408 weather stations in China that has complete time series from 2013 to 2016. We match each city to the nearest weather station in ISD using their geographical coordinates. All timestamps in the dataset are adjusted by an 8-hour lead to offset the difference between Bejing Time and Greenwich Mean Time. We average over hourly readings to obtain the daily average temperature.

HSR Network The expansion of the HSR network has been unprecedented in China (Figure A1). While the country had no HSR at the beginning of 21st century, the total lengthen of HSR reached 37,900 km by 2020, linking all of its major cities. The rapid expansion of the HSR network has led to one of the most significant increases in human mobility in modern history: the passenger trips via HSR increased from 290 million to 2.3 billion during 2010-2019.

We gather information on the opening dates of HSR station from government official reports. If a city has multiple HSR stations, we use the date when the first HSR station started operation in the city. For HSR connections, we use national railway timetables which report the origin and destination cities for all train services on a given day. The number of connections via HSR is defined as the number of distinct cities that are directly connected to the origin city via HSR. China's airport

network also expanded during our sample period. To control for the expansion of the air transport network, we collect data on airport connections based on monthly reports from the Official Aviation Guide that cover schedules on all of China's domestic flights from 2013 to 2016.

Figure 1 provides the first descriptive evidence on the benefit of improved transportation networks in mitigating households' pollution exposure. The top panel plots travelers' pollution exposure against the corresponding day's pollution in the home city. Travelers' pollution exposure is defined as the weighted average of the daily pollution levels across destination cities, where the weights are daily origin-destination traveler shares. Travelers based in cities with active HSR connections experience a statistically significant lower pollution exposure than those without HSR connections throughout the entire spectrum of home pollution levels, with a widening gap as home conditions deteriorate. When the home city suffers from hazardous pollution – $PM_{2.5}$ higher than 100 $\mu g/m^3$ (the 90^{th} percentile), the wedge between travelers from HSR cities and those from non-HSR cities exceeds 9 $\mu g/m^3$ and can reach as high as 30 $\mu g/m^3$.

Table 1 provides the second piece of descriptive evidence by further tabulating travel patterns – the share of traveler flows to destination cities with different pollution quintiles – for each pollution quintile of the home city. Panels (a) and (b) present the statistics for HSR city travelers and non-HSR city travelers, respectively, and Panel (c) reports their difference. Consistent with the evidence in Figure 1, the last column of Panel (c) shows that intercity travelers from cities with HSR access experience a lower pollution exposure than travelers from cities without HSR across all five quintiles of home pollution. The gap increases monotonically with home pollution levels. While the difference is a modest 0.44 μg/m^3 when the home city's pollution is in the lowest quintile, the gap enlarges to 8.35 μg/m^3 at the highest quintile. Much of this reduction is driven by a noticeably smaller fraction of HSR city travelers who visit dirty destinations (47.3%) than non-HSR city travelers (55.1%).

Appendix Table A1 and Section A provide the summary statistics of key variables and additional descriptive evidence. Results for temperature exposure are similar and are shown in Appendix Figure A3 and Table A2. These patterns present strong suggestive evidence that travelers benefit from improvements in passenger transportation infrastructure by experiencing reduced exposure to adverse environmental conditions.

3 Empirical Framework

Our empirical framework combines the difference-in-differences (DID) and triple-differences to examine how improved transportation infrastructure affects travelers' exposure to environmental

extremes:

$$TravExpo_{it} = \beta_1\ Expo_{it} + \beta_{2i} HSR_{it} + \beta_3 HSR_{it} \times Expo_{it} + X_{it} + \mu_i + \delta_t + \varepsilon_{it}. \tag{1}$$

The outcome variable of our analysis, travelers' exposure, $TravExpo_{it}$ captures the average exposure to environmental (either air pollution or temperature) extremes for travelers from city i on day t. It is defined as a weighted average of environmental conditions at the destination cities, where the weight for a destination city is the share of travelers from a given city to the corresponding destination city:

$$TravExpo_{it} = \sum_{j \neq i} Expo_{jt} \cdot \frac{N_{ijt}}{\sum_{k \neq i} N_{ikt}}, \tag{2}$$

where $Expo_{jt}$ is the environmental condition in destination city j on day t, N_{ijt} is the number of travelers from city i visiting city j on day t, and $\sum_{k \neq i} N_{ikt}$ is the total number of travelers from city i on day t. In our baseline specification, $Expo_{jt}$ is constructed as an indicator being one when city i experiences extreme air pollution or temperature on day t. Extreme pollution is defined as $PM_{2.5}$ larger than 100 μg/m^3 (the 90th percentile of the empirical distribution) and extreme temperature is defined as daily average temperature below 30°F or above 90°F (about 10% of the observations).[4] In robustness checks, we use different cutoffs to define extreme conditions and also estimate a model with continuous environmental variables.

HSR_{it} captures the connectivity of city i at time t. We use two measures: an indicator variable indicating whether city i is connected to the network or not at time t, and a continuous connectivity measure that is a weighted number of destination cities that can be reached from city i via HSR at time t. The weight for each destination city j is its total inflow of visitors in the base year of 2012 over the squared distance between the origin and destination city-pair:

$$\begin{aligned} \widetilde{HSR^C_{it}} &= \sum_{j \neq i} \left[\frac{TotalInflow_{j,2012}}{Distance^2_{ij}} \times HSR_{ijt} \right], \\ HSR^C_{it} &= (\widetilde{HSR^C_{it}} - \mu)/\sigma. \end{aligned}$$

$TotalInflow_{j,2012}$ is city j's total number of visitors in 2012, $distance_{ij}$ is the great circle distance, and HSR_{ijt} is an indicator for HSR connection between city-pair ij on date t. We normalize the connectivity measure to have zero mean and unit variance and define it as HSR^C_{it}. Unlike the HSR dummy (HSR_{it}) used in the main analysis whose value remains the same after a city is first connected

[4] China's standard for daily maximum $PM_{2.5}$ is 75 μg/m^3. In comparison, the US Environmental Protection Agency's daily $PM_{2.5}$ standard is 35 $\mu g/m^3$.

to the HSR network, HSR_{it}^{C} increases whenever city i is connected to additional destinations as the HSR network expands. In addition, this measure also reflects cities' centrality in the transportation network.

The coefficient β_1 in Equation (3) captures the relationship between a home city's environmental condition and its travelers' exposure. While both pollution and temperature are correlated geographically, the spatial correlation decays across space. In the absence of a strong correlation between the trip direction and destination conditions (e.g., all trips going from dirty to dirty cities), one should expect to see $0 < \beta_1 < 1$. The second coefficient, β_{2i}, varies by city and allows for differential changes in travelers' exposure before and after the HSR connection. The key parameter of interest is β_3 on the interaction term, $HSR_{it} \times Expo_{it}$. It captures how HSR connection affects the slope of the relationship between local environmental conditions and travelers' exposure. If HSR facilitates residents' ability to mitigate adverse environmental conditions at home, β_3 should be negative. Time-varying city attributes X_{it} include whether city i has airports at time t and the number of destination airports with direct flights from city i. We incorporate city fixed effects μ_i to control for time-invariant unobservables (e.g., connectivity or centrality) at the city level and day-of-sample fixed effects δ_t to absorb seasonality and temporal shocks in travel patterns.[5]

The identification of β_{2i} relies on the DID strategy and the staggered roll-out of the HSR expansion across cities. The identification of β_3 relies on a triple-difference design: it compares changes in the outcome variable (before and after the HSR connection) when the home city is subject to environmental extremes relative to changes in the outcome when the home city has mild environmental conditions. As illustrated in both Figure 1 and Panel (c) in Table 1, when home city is clean, travelers from cities with HSR connection experience a negligible or small reduction in pollution exposure compared to those from cities without HSR connection. However, when home city is polluted, the reduction in pollution exposure is much more pronounced. The differences in the pollution exposure reduction across different pollution levels in the home city pin down the magnitude of β_3.

The key identification assumption is that the exact timing of a city's connection to the HSR network is exogenous. That is, there are no confounding factors that affect the relationship between a home city's environmental conditions and its travelers' exposure before and after the HSR connection. The assumption would be violated if the connection is driven by or in response to time-varying and city-specific unobservables that also affect travel patterns hence travelers' exposure to environmental extremes.

In practice, the HSR network's expansion is a complicated process involving many entities and numerous steps including siting, obtaining building permissions, securing the financing, and imple-

[5] All regressions are weighted by the number of travelers from home city i on day t, so that the effect sizes reported below can be interpreted as the national average across all travelers.

menting the physical construction. The exact timing (day or month) of a city's connection to the HSR network is often driven by a host of idiosyncratic factors. Most HSR lines in our sample began construction in 2005 or right after 2008, directly following the passage of the Mid-to-Long Term Railway Network Plan in 2004 and its revision in 2008. However, their completion dates spread out across years. The duration of the construction progress depends on engineering difficulties which increases with the railway's length and bridge/tunnel ratio. For instance, the opening of the Wuhan-Guangzhou line must wait for the completion of the Wuhan Tianxingzhou Yangtze River Bridge, the longest combined road and rail span bridge in the world. It is also affected by political factors, accidents, and other exogenous factors that expedite or delay these projects. Notable examples include the Wenzhou train crash in July 2011 that has halted the construction of ongoing projects for more than a year.[6]

The event study in Figure 2 displays no clear trend in changes in travelers' exposure to extreme pollution on either clean or polluted days before the HSR connection, lending support to our identification assumption. In addition, the HSR treatment effects appear stable over time, which suggests that our estimates are less subject to the concerns on two-way fixed effects regressions when treatment effects are dynamic (evolving over time) and the inclusion of early-treated units in the control group (Goodman-Bacon, 2021).

All regressions are weighted by the number of home city i's travelers at time t, so that the effect sizes reported below can be interpreted as the national average across all travelers.[7] In theory, if HSR connection simply enables travelers to travel further to destinations whose pollution and temperature are less correlated to those at home, the aggregate benefit in terms of pollution mitigation could be either negative or positive. For example, travelers might visit dirty places when home cities are clean. This negative effect could cancel out or dominate the benefit from mitigation when the home city is polluted. Hence, whether improved transportation facilitates adaptation on net is an empirical question.

[6] https://www.ft.com/content/a9337b06-fe20-11e0-a1eb-00144feabdc0

[7] The aggregate benefit of the HSR network's expansion on travelers' pollution exposure is estimated based on $-\sum_i \sum_t \omega_{it}(\beta_{2i} + \beta_3 \times Expo_{it})$, where ω_{it} is the share of travelers in city i and on day t among all HSR city-days in our sample period.

4 Empirical Findings

4.1 Baseline Results

Table 2 reports OLS estimates as specified in Equation (3) for travelers' exposure to air pollution and temperature in Panel (a) and (b), respectively. Column (1) uses the indicator variable to measure HSR connectivity while Column (2) uses the continuous measure. The estimates of β_1 in both columns and both panels are significantly lower than one, implying that intercity travel reduces the correlation between the environmental condition in the home city and travelers' realized exposure. The estimates of β_1 for temperature exposure are slightly larger than those for pollution exposure, likely due to stronger spatial correlation in temperature than air pollution.

The estimates of β_{2i}, not shown in the table, tend to be small and statistically insignificant on average, consistent with the negligible differences in the two lines' intercept as shown in Figure 1. In Column (1) for example, the set of β_{2i} estimates has an average of -0.002 and standard error of 0.033 for air pollution, and an average of 0.008 and standard error of 0.018 for temperature.[8]

In contrast to the small estimates of β_{2i}, the estimates of β_3 are negative and economically large in all columns. In other words, the impact of HSR connection on adaptation is mainly through the change in the slope, rather than the intercept. As a result, the expansion of the HSR network has flattened the relationship between environmental extremes in the home city and travelers' exposure.

The last row of Panel (a) presents the HSR connection's aggregate impact across all city-days on travelers' exposure to environmental extremes. HSR connection leads to a 0.7 percentage-point reduction in the likelihood of being exposed to extreme pollution (relative to the sample mean of 11 percentage points), based on the discrete measure of HSR connectivity. This represents a 7% decrease in travelers' likelihood of experiencing extreme pollution over all environmental conditions in home cities. Using the continuous measure, HSR connectivity leads to a 1.1 percentage-point reduction, or 10% decrease in travelers' exposure to extreme pollution. The larger estimates reflect the continuous measure's ability to capture not only the home city's connection to the HSR network, but also the improved connectivity as the network expands.

Results on travelers' exposure to extreme temperatures are reported in Panel (b). These findings mirror those for pollution exposure: intercity travel reduces the correlation between home conditions and travelers' realized exposure. In addition, connection to a better passenger transportation network reduces travelers' likelihood of exposure to extreme temperatures by 0.6 percentage points (using the discrete HSR connection measure) and 0.7 percentage points (using the continuous HSR connection measure) out of a sample mean of 6 percentage points, which is equivalent to a 10-11% reduction.

[8]The inter-quartile range is from -0.015 to 0.020 for pollution and from 0.003 to 0.020 for temperature.

Figure 3 illustrates the magnitude of the estimates in Column (1) of Table 2 by contrasting the actual exposure to extreme conditions with counterfactual exposure for travelers with HSR connections. The counterfactual exposure is simulated as the predicted outcome from Equation (3) when HSR dummies are switched to zero. This comparison allows us to focus on the same set of city-days with HSR connections and avoid the differences between HSR cities and non-HSR cities that are unrelated to pollution mitigation. Panels (a) and (b) display results for pollution exposure and temperature exposure separately.

When a traveler's home city is clean, the traveler can expect to experience a modest chance (8 percentage points) of being subject to severe pollution – a reflection of mean reversion and the spatial heterogeneity of air pollution. Removing HSR only moderately increases the traveler's chance of experiencing severe pollution to 8.1 percentage points. In contrast, when the home city is suffering from extreme pollution, removing access to the HSR network would raise the traveler's probability of experiencing extreme pollution from 38.4 to 43.3 percentage points, amounting to a 12.8% increase. Results for extreme temperature exposure are similar. The impact of HSR connection is negligible when home cities have mild temperatures. But when home cities are subject to extreme temperatures, removing HSR would increase travelers' exposure to such extremes from 38.6 to 49.3 percentage points, a 27.7% jump.

4.2 Robustness Checks

This section explores the robustness of our findings to alternative specifications. Table A3 reports a host of robustness checks for both the discrete measure of HSR connectivity (Panel (a)) and continuous measure of HSR connectivity (Panel (b)). In Columns (1) and (2), we replace the indicator of extreme pollution with the continuous PM2.5 reading and replace the indicator of extreme temperature with the absolute deviation from 70°F. One $\mu g/m^3$ increase in $PM_{2.5}$ at home translates into 0.34 $\mu g/m^3$ increase in travelers' exposure for cities not connected to HSR and only 0.28 $\mu g/m^3$ for travelers from HSR cities, using the discrete measure of HSR connectivity. The patterns are similar for the effect on temperature exposure. Columns (3)-(6) use alternative cutoffs to define environmental extremes: Columns (3) and (4) use 120 $\mu g/m^3$ and 150 $\mu g/m^3$ for extreme pollution, Column (5) uses 25 $^\circ F$ and 95 $^\circ F$ as the cutoffs for extreme temperature, and Column (6) uses 35 $^\circ F$ and 85 $^\circ F$ for the temperature cutoff. The coefficient estimates have the same signs and are similar in magnitude to the baseline estimates in Table 2. Results are similar using the continuous measure of HSR connectivity.

Table A4 examines robustness to different sample cuts for both the discrete (Panel (a)) and continuous measures (Panel (b)) of HSR connectivity. The number of travelers in our analysis

is derived from card transactions and subject to measurement errors. To examine robustness to potential measurement errors, Columns (1) and (2) exclude each city's 5% of days with the most card transactions and 5% of days with the least card transactions. Columns (3) and (4) exclude 10% of days with the most and 10% of days with the least transactions. In addition, since card penetration rates are lower in small cities, Columns (5) and (6) only keep the large cities defined in the top three tiers. There are 117 cities in the top three tiers out of a total of 336 cities. These cities have larger populations than the lower-tier cities and account for over 80% of travelers in our sample. All of these regressions demonstrate that our results are robust to measurement errors and that the expansion of the passenger transportation infrastructure makes the intercity travel an effective strategy to reduce exposure to environmental extremes.

Our specifications so far relate travelers' exposure to home conditions on the same day. This implicitly assumes that households can respond quickly to negative shocks. Given the easy access to pollution and weather forecasts during our sample period, and the expansive train network and frequent services, households can and often do use forecasts to travel to desirable places in the event of (anticipated) pollution episodes and heat waves (Arlt, 2017; Sharkov, 2016; Chen et al., 2021).

Nonetheless, to allow for the possibility that households react with a lag to pollution and temperature shocks (due to the time constraint it takes to respond) or respond in advance of these shocks (due to the wide availability and increasing accuracy of forecasts), Table A5 replaces the daily environmental measure $Expo_{it}$ with its average in the following week in Column (1) and with its average in the previous week in Column (2). Similar to Tables A3-A4, Panel (a) presents results using the discrete HSR connectivity and Panel (b) reports results using continuous connectivity. Travelers respond to both leading and lagged home pollution/temperature, though the magnitudes are smaller than responses to contemporary conditions. These results suggests that HSR facilitates adaptation to both contemporaneous environmental shocks and recent and future shocks.

5 Channels of Impacts and the Extensive Margin

5.1 Channels of Impacts

Changes in Travel Distance HSR access reduces travel costs, expands the set of feasible destinations, and allows individuals to travel to more distant destinations. Panels (a) and (b) of Appendix Figure A4 plot the distribution of trip distance for travelers from cities with and without HSR connection. As the associated benefit is more pronounced when a traveler's home city experiences high pollution as shown above, we plot the distributions separately for clean and polluted days (with $PM_{2.5}$ exceeding 100 $\mu g/m^3$). Panel (c) presents the difference in trip distances between travelers

from HSR cities and those from non-HSR cities during days that are polluted (red bars) and clean (green bars). HSR connection has significantly shifted the travel distribution to the right: the fraction of trips exceeding 500 km increases from 35% among travelers without HSR connection to 52% among those with access when home cities are clean. The difference in the fraction of trips exceeding 500 km is even more pronounced and widens to 21 percentage points during polluted days.

These patterns suggest that HSR expansion allows people to travel farther. As correlations in environmental conditions decay spatially, traveling farther reduces travelers' probability of experiencing adverse conditions similar to those observed at home. Can distance alone explain the entirety of HSR's mitigation effect? To answer this question, we replace the environmental conditions at destination cities with the concurrent environmental conditions in cities that are of a similar distance to the origin in the construction of travelers' exposure:[9]

$$TravExpo^1_{it} = \sum_{j \neq i} \widehat{Expo_{jt}} \cdot \frac{N_{ijt}}{\sum_{k \neq i} N_{ikt}},$$

where $\widehat{Expo_{jt}}$ is the pollution level of a randomly-chosen city that is similarly distant from the original city as city j on the same day t. We simulate this alternative traveler exposure $TravExpo^1_{it}$ for all origin cities and all days in the sample. Then we use this alternative measure of travelers' exposure as the outcome variable in equation (3).

We replicate this simulation exercise 100 times and report results in the top panel of Table A6.[10] This analysis preserves the distribution of travel distance for all cities. If distance is the only channel underlying HSR's mitigation effect, we should expect estimates from these simulations to be close to those using real data. Instead, HSR's coefficients center around -0.02 and -0.06 for pollution and temperature exposure, respectively, and are much smaller in absolute value than the baseline estimates of -0.05 and -0.12 in Table 2. Correspondingly, the aggregate benefit of HSR in this simulation exercise is only a 0.3 percentage point reduction in exposure to extreme pollution and extreme temperatures. This constitutes 43% of HSR's baseline effects for pollution mitigation and 50% of HSR's baseline effects for temperature mitigation. We conclude that distance-based factors cannot explain all of HSR's mitigation benefits documented in the main text. Instead, travelers appear to be able to leverage HSR connection and deliberately choose destination cities with better

[9] We allow for a maximum difference of 100 km when defining cities of similar distance to the origin. Specifically, for each origin-destination pair, we draw a circular band centering around the origin, with the inner and outer radius being the distance between the city pair ± 100 km. One of the cities within the band is randomly picked and its pollution level of the day is used as the counterfactual.

[10] The reported β's are the average estimates from the simulation runs, and their standard errors are directly calculated using the simulation estimates.

environmental conditions, conditioning on the distance to the origin city.

Adaptation Horizons Adaptation to environmental extremes through intercity travel could arise from multiple margins. First, individuals can travel to places with predictably desirable environmental conditions, such as trips to southern cities during polluted and harsh winter months in northern cities. Second, residents can spontaneously evade unexpected environmental extremes at home by visiting cities with better environmental conditions. Both margins of adjustment are associated with reduced exposure to environmental extremes and could generate mortality and morbidity benefits, though the second margin has shorter (planning) horizons than the first one. The changes in travel behavior as illustrated in Appendix Figure A4 are consistent with both margins. This section presents simulations that disentangle these different margins.

To quantify the benefit of HSR that derives from longer horizon responses to predictable environmental extremes as distinct from short horizon adaptation to unpredicted environmental conditions, we use the average shares of each home city's travelers visiting different destinations to construct the travelers' exposure, instead of the daily travel shares. We do this separately for before and after the HSR connection:

$$TravExpo_{it}^{2} = \sum_{j \neq i} Expo_{jt} \cdot \frac{N_{ij}^{\text{No HSR}}}{\sum_{k \neq i} N_{ik}^{NoHSR}} \cdot \mathbb{1}\{t \text{ before HSR}\} + \sum_{j \neq i} Expo_{jt} \cdot \frac{N_{ij}^{\text{HSR}}}{\sum_{k \neq i} N_{ik}^{HSR}} \cdot \mathbb{1}\{t \text{ post HSR}\},$$

where $N_{ij}^{\text{No HSR}}$ is the total number of travelers from city i to city j prior to the HSR access and N_{ij}^{HSR} is the total number of travelers from city i to city j post the HSR access. By construction, this formulation removes deliberate travel responses to temporal, day-to-day variations in environmental conditions. Then we use this alternative measure of travelers' exposure as the outcome variable in Equation (3). The lower panel of Appendix Table A6 suggests that this margin accounts for 71% of HSR's aggregate benefit in pollution mitigation and 83% for temperature. We attribute the remaining benefit (29% of pollution reduction and 17% of temperature mitigation) to day-to-day avoidance behavior, whereby residents deliberately seek cities with better environmental conditions when the home city is hit by unpredicted environmental extremes. HSR access has a relatively smaller impact on day-to-day temperature mitigation than pollution mitigation because temperature extremes exhibit less geographical variation and hence are harder to escape from.

5.2 The Extensive Margin

Our analysis has so far focused on the intensive margin of travel responses: the role of HSR in helping travelers escape pollution and temperature extremes on a short-term basis. However, adjustments

at the extensive margin could also be relevant. It is unclear ex-ante whether people travel more or less when the home city experiences environmental extremes and how HSR affects the extensive margin. On the one hand, people might have stronger incentives to travel to cities that are cleaner or with more moderate temperatures as a means of avoidance. On the other hand, people might reduce outdoor activities entirely, thus limiting their intercity travel. Appendix Table A7 reports results from a Poisson pseudo maximum likelihood (PPML) regression using the number of outbound travelers in a city-day as the outcome variable.[11] Consistent with the findings in the literature (Moretti and Neidell, 2011b; Graff Zivin and Neidell, 2014; Barwick et al., 2018), residents travel less when their home cities are subject to extreme conditions. This is in line with the observation that residents stay indoors to avoid exposure, as advocated by the government and news media. On the other hand, having access to the HSR network increases the number of outbound trips by 4-5% (first row) and facilitates travel during episodes of environmental extremes, especially on polluted days (columns 2-3).

We also conduct another analysis that directly looks at the impact of HSR on monthly outbound travelers. To address the potential treatment effect heterogeneity in the staggered DID design, Figure A7 plots the event study of HSR opening on the share of outbound travelers among a city's population following the strategy proposed in Callaway and Sant'Anna (2021) and Sant'Anna and Zhao (2020). There was no clear pre-trend before HSR opening, lending credence to the randomness of the treatment timing. However, there was a pronounced jump after the opening: having HSR access leads to a 0.013 percentage point increase in the share of travelers (i.e. roughly a 5% increase from the base of 0.28 percentage points). These two pieces of evidence are consistent in suggesting that despite a contraction of travelling in extreme conditions, HSR promotes outbound trips by around 5% in both polluted and non-polluted days.

6 Health Benefits

Our analysis shows that the HSR access leads to a 0.7 percentage point reduction in travelers' likelihood of experiencing extreme pollution (Table 2), or a 7% reduction in travelers' average pollution exposure. This is equivalent to an annual reduction of 3.9 $\mu g/m^3$ $PM_{2.5}$ in pollution exposure for an average traveler. Based on Ebenstein et al. (2017)'s mortality estimates from air pollution and the value of statistic life for a Chinese traveler, the annual reduction in pollution exposure induced by

[11] PPML models (Silva and Tenreyro, 2006) are commonly used in the trade and migration literature. It is preferred to OLS (log-)linear specification in our setting for its consistency in the presence of heteroskedasticity and large dispersion in the outcome variable.

improved HSR transportation networks translates to a nationwide savings of $2.2 billion in 2015.[12]

For the mortality impact of temperature extremes, we follow the age-specific dose-response functions from Deschênes and Greenstone (2011). Applying their estimates to the age structure of the Chinese population, one-day less exposure to temperature extremes decreases the mortality rate by 4.6 to 8.6 per million people, with the elderly population accounting for the lion's share of the benefit. The expansion of HSR network reduces an average travelers' exposure to temperature extremes by two days per year (Table 2). Taken together, these estimates suggest that mitigation in exposure to temperature extremes as a result of the HSR expansion leads to an annual savings of $532 million to $944 million in mortality cost.

Overall, the mortality benefit from the moderation in population exposure to air pollution and temperature extremes as a result of the HSR network expansion amounts to $2.7 billion to $3.1 billion per year at the national level. Deschênes et al. (2017) and Barwick et al. (2018) show that the morbidity benefit can be as high as two-thirds of the mortality benefit from reduced air pollution in the U.S. and China, respectively. If morbidity savings were included, the aggregate health benefit could amount to $4.5 to $5.1 billion per year.

7 Conclusion

The role of human mobility especially in the form of short-term migration as an adaption strategy to a changing environment is not well understood. This study examines whether improved transportation infrastructure could promote short-term mobility and facilitate behavioral changes in response to adverse environmental conditions. The empirical analysis benefits from high-frequency data on intercity travels, China's massive and staggered expansion of the HSR network, as well as rich variation in daily pollution and temperature at the city level.

Our analysis finds that the rapid expansion of HSR has made short-term intercity passenger travel an effective adaptation strategy to adverse environmental conditions, leading to significant health benefits. Such adaptation can be attributed to both short-run deliberate responses to unexpected environmental extremes at home and also shifts in longer-term travel patterns due to reduced travel costs. These findings contribute to our understanding of the role of adaptation and the benefit of transportation infrastructure investment in a changing environment. Examining the potential

[12] Ebenstein et al. (2017)'s mortality estimates refer to PM_{10}. As shown by China's pollution monitoring data, one $\mu g/m^3$ increase in $PM_{2.5}$ corresponds to 1.5 $\mu g/m^3$ increase in PM_{10}. We multiply Ebenstein et al. (2017)'s mortality estimates by 1.5 to derive the impact of $PM_{2.5}$ exposure in our context. Based on the transfer elasticity of 1.2 and the U.S. population's VSL estimate at 2.27 million in 2015$ from Ashenfelter and Greenstone (2004), the estimated VSL for the Chinese population is $0.21 million for a prime age person. Our results are age-adjusted based on Murphy and Topel (2006).

feedback effects of these behavioral changes on air pollution and carbon emissions is an important topic for future research.

References

Agrawal, Ajay, Alberto Galasso, and Alexander Oettl, "Roads and innovation," *Review of Economics and Statistics*, 2017, *99* (3), 417–434.

Arlt, Wolfgang Georg, "As Smog Hits China, Chinese Tourists Seek Fresh Air On Pollution Free Holidays," *Forbes*, Jan 2017.

Ashenfelter, Orley and Michael Greenstone, "Using Mandated Speed Limits to Measure the Value of a Statistical Life," *Journal of Political Economy*, 2004, *112*, S226–67.

Balboni, Clare, "In Harm's Way? Infrastructure Investments and the Persistence of Coastal Cities," 2021. Working Paper.

Banzhaf, H. Spencer and Randall P. Walsh, "Do People Vote with Their Feet? An Empirical Test of Tiebout," *American Economic Review*, 2008, *98*, 843–863.

Barreca, Alan, Karen Clay, Olivier Deschênes, Michael Greenstone, and Joseph S Shapiro, "Adapting to climate change: The remarkable decline in the US temperature-mortality relationship over the twentieth century," *Journal of Political Economy*, 2016, *124* (1), 105–159.

Barwick, Panle Jia, Shanjun Li, Deyu Rao, and Nahim Bin Zahur, "The morbidity cost of air pollution: evidence from consumer spending in China," 2018.

_ , _ , Liguo Lin, and Eric Zou, "From Fog to Smog: the Value of Pollution Information," 2020.

Baum-Snow, Nathaniel, "Changes in transportation infrastructure and commuting patterns in US metropolitan areas, 1960-2000," *American Economic Review*, 2010, *100* (2), 378–82.

Bayer, Patrick, Nate Keohane, and Christopher Timmins, "Migration and Hedonic Valuation: The Case of Air Quality," *Journal of Environmental Economics and Management*, 2009, *58*, 1–14.

Behrens, Christiaan and Eric Pels, "Intermodal competition in the London–Paris passenger market: High-Speed Rail and air transport," *Journal of Urban Economics*, 2012, *71* (3), 278–288.

Bernard, Andrew B, Andreas Moxnes, and Yukiko U Saito, "Production networks, geography, and firm performance," *Journal of Political Economy*, 2019, *127* (2), 000–000.

Black, Richard, Stephen RG Bennett, Sandy M Thomas, and John R Beddington, "Climate change: Migration as adaptation," *Nature*, 2011, *478* (7370), 447.

Burke, Marshall B, Edward Miguel, Shanker Satyanath, John A Dykema, and David B Lobell, "Climate robustly linked to African civil war," *Proceedings of the National Academy of Sciences*, 2010, *107* (51), E185–E185.

Callaway, Brantly and Pedro HC Sant'Anna, "Difference-in-differences with multiple time periods," *Journal of Econometrics*, 2021, *225* (2), 200–230.

Carleton, Tamma A and Solomon M Hsiang, "Social and economic impacts of climate," *Science*, 2016, *353* (6304), aad9837.

Chen, Shuai, Paulina Oliva, and Peng Zhang, "The Effect of Air Pollution on Migration: Evidence from China," 2017. NBER Working Paper No. 24036.

_ , Yuyu Chen, Ziteng Lei, and Jie-Sheng Tan-Soo, "Chasing Clean Air: Pollution-Induced Travels in China," *Journal of the Association of Environmental and Resource Economists*, 2021, pp. 59–89.

Chen, Yuyu, Avraham Ebenstein, Michael Greenstone, and Hongbin Li, "Evidence on the impact of sustained exposure to air pollution on life expectancy from China's Huai River policy," *Proceedings of the National Academy of Sciences*, 2013, *110*, 12936–12941.

Cruz, José-Luis and Esteban Rossi-Hansberg, "The Economic Geography of Global Warming," 2021. Working Paper.

Currie, Janet and Matthew Neidell, "Air Pollution and Infant Health: What Can We Learn from California's Recent Experience," *Quarterly Journal of Economics*, 2005, *120*, 1003–1030.

Dell, Melissa, Benjamin F Jones, and Benjamin A Olken, "Temperature shocks and economic growth: Evidence from the last half century," *American Economic Journal: Macroeconomics*, 2012, *4* (3), 66–95.

Deschênes, Olivier and Enrico Moretti, "Extreme weather events, mortality, and migration," *The Review of Economics and Statistics*, 2009, *91* (4), 659–681.

_ **and Michael Greenstone**, "Climate Change, Mortality, and Adaptation: Evidence from Annual Fluctuations in Weather in the US," *American Economic Journal: Applied Economics*, October 2011, *3* (4), 152–185.

_ **,** _ **, and Jonathan Guryan**, "Climate Change and Birth Weight," *American Economic Review*, May 2009, *99* (2), 211–217.

_ **,** _ **, and Joseph Shapiro**, "Defensive Investments and the Demand for Air Quality: Evidence from the NOx Budget Program," *American Economic Review*, 2017, *107* (10), 2958–89.

Desmet, Klaus, Robert E. Kopp, Scott A. Kulp, Dávid Krisztián Nagy, Michael Oppenheimer, Esteban Rossi-Hansberg, and Benjamin H. Strauss, "Evaluating the Economic Cost of Coastal Flooding," *American Economic Journal: Macroeconomics*, April 2021, *13* (2), 444–86.

Donaldson, Dave, "Railroads of the Raj: Estimating the impact of transportation infrastructure," *American Economic Review*, 2018, *108* (4-5), 899–934.

_ **and Richard Hornbeck**, "Railroads and American economic growth: A market access approach," *The Quarterly Journal of Economics*, 2016, *131* (2), 799–858.

Dong, Xiaofang, Siqi Zheng, and Matthew E Kahn, "The Role of Transportation Speed in Facilitating High Skilled Teamwork," *Journal of Urban Economics*, 2020.

Ebenstein, Avraham, Maoyong Fan, Michael Greenstone, Guojun He, and Maigeng Zhou, "New evidence on the impact of sustained exposure to air pollution on life expectancy from China's Huai River Policy," *Proceedings of the National Academy of Sciences*, 2017, *114*, 10384–10389.

Faber, Benjamin, "Trade integration, market size, and industrialization: evidence from China's National Trunk Highway System," *Review of Economic Studies*, 2014, *81* (3), 1046–1070.

Freeman, Richard, Wenquan Liang, Ran Song, and Christopher Timmins, "Willingness to pay for clean air in China," *Journal of Environmental Economics and Management*, 2019, *94*, 188–216.

Goodman-Bacon, Andrew, "Difference-in-differences with variation in treatment timing," *Journal of Econometrics*, 2021.

Greenstone, Michael, Guojun He, Shanjun Li, and Eric Zou, "China's War on Pollution: Evidence from the First Five Years," *Review of Environmental Economics and Policy*, 2021, *summer.* Forthcoming.

Hsiang, Solomon M, Marshall Burke, and Edward Miguel, "Quantifying the influence of climate on human conflict," *Science*, 2013, *341* (6151), 1235367.

Ito, Koichiro and Shuang Zhang, "Willingness to Pay for Clean Air: Evidence from Air Purifier Markets in China," *Journal of Political Economy*, 2020, *128*, 1627–1672.

Kahn, Matthew, *Climatopolis: How Our Cities will Thrive in Our Hotter Future*, Basic Books, 2010.

Landrigan, Philip, Richard Fuller, Nereus J R Acosta, Olusoji Adeyi, Maureen Cropper, Alan Krupnick, Michael Greenstone, and et al., "The Lancet Commission on pollution and health," *The Lancet*, 2018, *391* (10119), 462–512.

Lin, Yatang, "Travel costs and urban specialization patterns: Evidence from China's high speed railway system," *Journal of Urban Economics*, 2017, *98*, 98–123.

Luo, Ming and Ngar-Cheung Lau, "Heat waves in southern China: Synoptic behavior, long-term change, and urbanization effects," *Journal of Climate*, 2017, *30* (2), 703–720.

Miller, Douglas L., "Event Study Models," 2021. Working Paper.

Moretti, Enrico and Matthew Neidell, "Pollution, health, and avoidance behavior evidence from the ports of Los Angeles," *Journal of human Resources*, 2011, *46* (1), 154–175.

_ **and** _ , "Pollution, Health, and Avoidance Behavior: Evidence from the Ports of Los Angeles," *Journal of Human Resources*, 2011, *46*, 154–175.

Murphy, Kevin M. and Robert H. Topel, "The Value of Health and Longevity," *Journal of Political Economy*, 2006, *114* (5), 871–904.

Nordhaus, William D, "Geography and macroeconomics: New data and new findings," *Proceedings of the National Academy of Sciences*, 2006, *103* (10), 3510–3517.

Sant'Anna, Pedro HC and Jun Zhao, "Doubly robust difference-in-differences estimators," *Journal of Econometrics*, 2020, *219* (1), 101–122.

Sharkov, Damien, "Smog in China Prompts Tide of Tourism Fleeing 'Airpocalypse:' Report," *Newsweek*, Dec 2016.

Silva, JMC Santos and Silvana Tenreyro, "The log of gravity," *The Review of Economics and statistics*, 2006, *88* (4), 641–658.

The Health Effects Institute, "State of Global Air," 2019.

Ye, Dian-Xiu, Ji-Fu Yin, Zheng-Hong Chen, You-Fei Zheng, and Rong-Jun Wu, "Spatial and temporal variations of heat waves in China from 1961 to 2010," *Advances in Climate Change Research*, 2014, *5* (2), 66–73.

Zhang, Junjie and Quan Mu, "Air pollution and defensive expenditures: Evidence from particulate-filtering facemasks," *Journal of Environmental Economics and Management*, 2018, *92*, 517–536.

Zheng, Siqi and Matthew E Kahn, "China's bullet trains facilitate market integration and mitigate the cost of megacity growth," *Proceedings of the National Academy of Sciences*, 2013, *110* (14), E1248–E1253.

_ and _ , "A new era of pollution progress in urban China?," *Journal of Economic Perspectives*, 2017, *31* (1), 71–92.

Zivin, Joshua Graff and Matthew Neidell, "Temperature and the allocation of time: Implications for climate change," *Journal of Labor Economics*, 2014, *32* (1), 1–26.

Figure 1: Travelers' exposure to $PM_{2.5}$ vs. home exposure

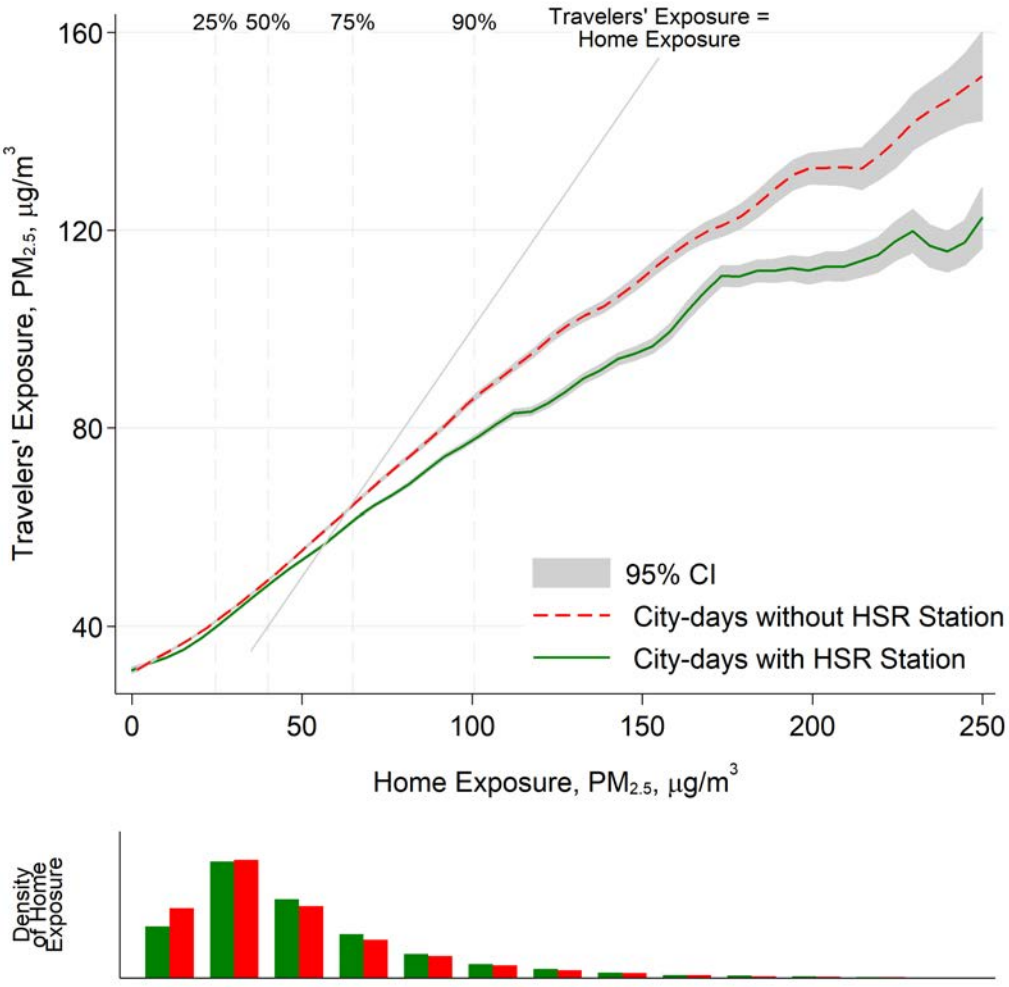

Notes: The top figure plots travelers' average exposure to $PM_{2.5}$ (y-axis) against $PM_{2.5}$ level at the travelers' home city (x-axis), separately for city-days with access to HSR (green line) and city-days without access to HSR (red dash line). Both lines are local polynomial regressions weighted by Epanechnikov kernel with optimal bandwidth. The gray area is the 95% confidence interval. Gray vertical lines mark the 25^{th}, 50^{th}, 75^{th}, and 90^{th} percentiles of the $PM_{2.5}$ distribution. The bottom figure displays the distribution of daily $PM_{2.5}$ at home cities, separately for city-days with access to HSR (green bars) and city-days without access to HSR (red bars).

Figure 2: Event study of HSR impact

(a) β_{2m}: impact of HSR on clean days

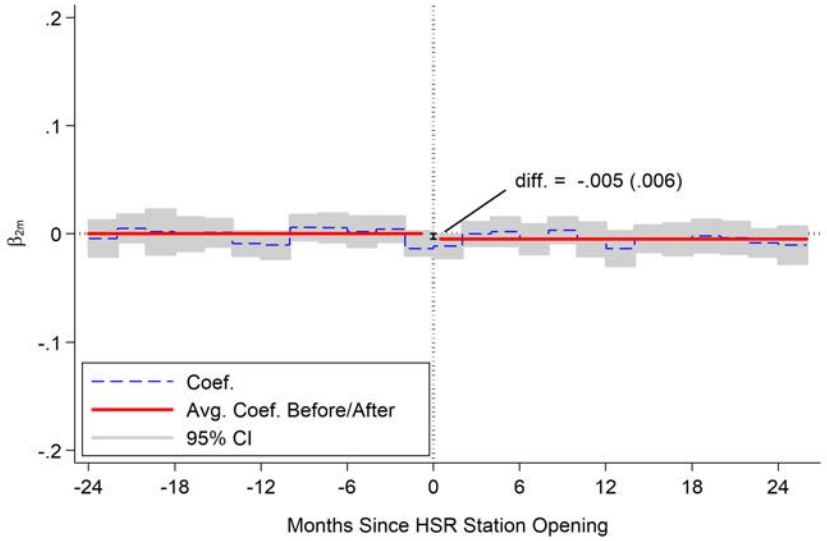

(b) β_{3m}: additional impact of HSR on polluted days

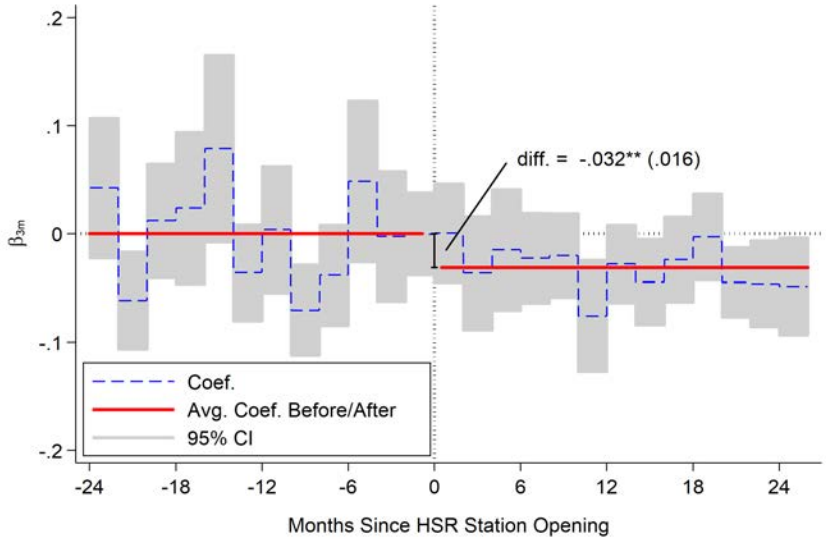

Notes: The figures plot coefficient estimates (blue dashed line) by month relative to HSR station openings from the following equation:

$$TravExpo_{it} = \beta_1 \, Expo_{it} + \sum_{m\in[-25,25]} \beta_{2m} HSR_{it} + \sum_{m\in[-25,25]} \beta_{3m} HSR_{it} \times Expo_{it} + X_{it} + \mu_i + \delta_t + \varepsilon_{it}, \tag{3}$$

where $TravExpo_{it}$ is exposure to extreme pollution for travelers from city i on day t. We group city-days that are more than 24 months before the HSR connection (including cities that are never connected) to $m = -25$ and city-days that are more than 24 months post the HSR connection to $m = 25$. The gray area denotes the 95% CI for the monthly coefficient estimates. The red line denotes the simple averages for months before and after the station opening. The bar denotes the difference between the two averages with its standard error in the bracket. We test the difference with a t-test and label the statistical significance with the following notations: *** $p < 0.01$, ** $p < 0.05$, and * $p < 0.10$. We normalize the average of the pre-opening coefficients to zero (instead of the coefficient on a single period to zero) following Miller (2021).

Figure 3: Access to HSR and reduction in exposure to pollution and temperature extremes

(a) Exposure to extreme pollution

(b) Exposure to extreme temperature

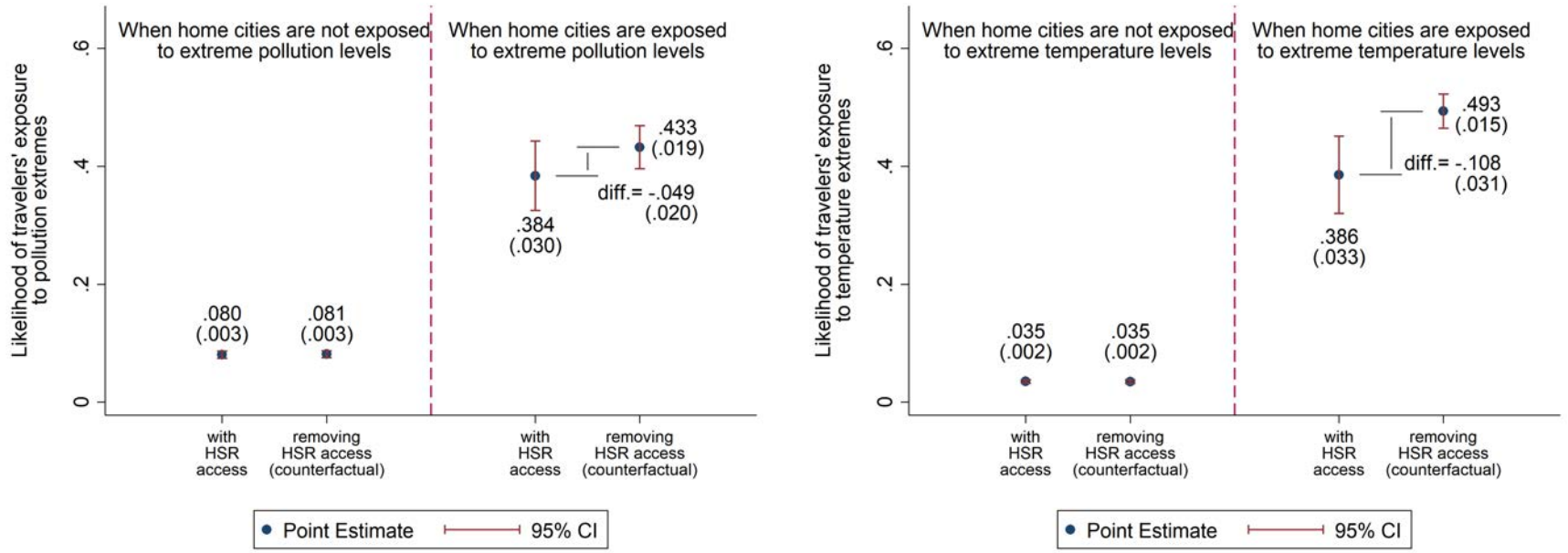

Notes: Actual and counterfactual likelihood of travelers experiencing extreme pollution (panel (a)) and extreme temperature (panel (b)), based on coefficient estimates in column (1) of Table 2. Dots to the left (right) of the red dashed line refer to days when home cities experience mild (extreme) conditions. Extreme pollution is defined as $PM_{2.5}$ above 100 $\mu g/m^3$ and extreme temperature is defined as daily average temperature below 30°F or above 90°F. Counterfactual exposure is the predicted outcome from Equation (3) when HSR dummies are switched to zero. Blue dots (whiskers) denote point estimates (95% confidence intervals). Standard errors in brackets are estimated from 100 block bootstrap replications with each home city as a block.

Table 1: Travelers' travel patterns and pollution exposure

(a) For travelers from city-days with HSR

		Flow shares by pollution quintile at destination					Avg. Exposure of $PM_{2.5}$ ($\mu g/m^3$) at	
		Clean 1	2	3	4	Dirty 5	Home	Dest.
Home in	Clean 1	40.1%	24.7%	15.4%	11.4%	8.4%	15.9	34.9
	2	23.4%	29.6%	21.6%	14.8%	10.7%	27.5	41.3
	3	14.7%	21.2%	27.5%	22.3%	14.2%	40.4	48.6
	4	10.5%	14.0%	21.6%	31.2%	22.6%	59.1	58.2
	Dirty 5	7.2%	9.8%	13.6%	22.0%	47.3%	120.0	83.8

(b) For travelers from city-days without HSR

		Flow shares by pollution quintile at destination					Avg. Exposure of $PM_{2.5}$ ($\mu g/m^3$) at	
		Clean 1	2	3	4	Dirty 5	Home	Dest.
Home in	Clean 1	37.0%	26.4%	17.2%	11.5%	7.9%	15.7	35.3
	2	21.1%	28.0%	23.5%	16.7%	10.8%	27.5	42.3
	3	13.0%	20.7%	27.4%	23.8%	15.2%	40.2	49.6
	4	8.5%	12.5%	21.0%	32.4%	25.7%	59.1	61.1
	Dirty 5	4.9%	7.3%	11.0%	21.8%	55.1%	115.4	92.2

(c) Difference between Panel (a) and Panel (b)

		Difference in flow shares by pollution quintile					Diff. in $PM_{2.5}$ ($\mu g/m^3$) at	
		Clean 1	2	3	4	Dirty 5	Home	Dest.
Home in	Clean 1	3.0%	-1.7%	-1.8%	-0.1%	0.5%	0.18	-0.44
	2	2.3%	1.6%	-1.8%	-1.9%	-0.1%	0.03	-1.03
	3	1.7%	0.5%	0.1%	-1.4%	-0.9%	0.14	-1.03
	4	2.1%	1.5%	0.7%	-1.2%	-3.1%	0.00	-2.92
	Dirty 5	2.3%	2.5%	2.6%	0.2%	-7.7%	4.61	-8.35

Notes: This table complements Figure 1 and illustrates that travelers from HSR cities are more likely to visit cleaner cities than those from non-HSR cities. Each row represents the shares of travels to destination cities with different pollution quintile, conditioning on the home city-day's pollution quintile. Panel (a) refers to travelers from city-days with HSR, panel (b) refers to travelers from city-days without HSR, and panel (c) presents the difference between the two. Positive (negative) values are colored in different shades of green (red) according to the magnitude. The quintile cutoffs for daily $PM_{2.5}$ are 22, 33, 48, and 73 $\mu g/m^3$.

Table 2: Travelers' likelihood of experiencing environmental extremes

	(1) Discrete HSR_{it}	(2) Continuous HSR_{it}
Panel (a) : Air Pollution Daily $PM_{2.5} > 100\mu g/m^3$	Likelihood of experiencing pollution extremes	
$\mathbb{1}\{\text{home extreme}\}$	0.27***	0.19***
	(0.01)	(0.01)
$\mathbb{1}\{\text{home extreme}\} \times HSR_{it}$	-0.05***	-0.04***
	(0.02)	(0.01)
N	330,801	330,801
R^2	0.79	0.79
HSR's overall impact	-0.007**	-0.011**
	(0.003)	(0.004)
Panel (b) : Temperature Daily temp. $< 30°$F or $> 90°$F	Likelihood of experiencing temperature extremes	
$\mathbb{1}\{\text{home extreme}\}$	0.40***	0.32***
	(0.03)	(0.01)
$\mathbb{1}\{\text{home extreme}\} \times HSR_{it}$	-0.12***	-0.07***
	(0.03)	(0.01)
N	466,257	466,257
R^2	0.79	0.79
HSR's overall impact	-0.006***	-0.007**
	(0.002)	(0.003)

Notes: All regressions are weighted by home cities' number of outbound travelers on day t. The dependent variable in Panel (a) and (b) is the likelihood that travelers experience extreme pollution ($PM_{2.5} > 100\mu g/m^3$) and extreme temperature (daily average temperature $< 30°$F or $> 90°$F), respectively, defined in Eq. (2). The average of the dependent variables for pollution and temperature is 0.11 and 0.06, indicating the likelihood of travelers being subject to extreme pollution and temperature of 11% and 6%. $\mathbb{1}\{\text{home extreme}\}$ is an indicator for extreme conditions at home city i on day t. In Column (1), HSR_{it} is the indicator variable for access to HSR stations in the home city. In Column (2), we instead use the standardized continuous connectivity measure, HSR^C_{it}. The number of observations is smaller in panel (a) as not all cities had $PM_{2.5}$ monitoring stations in 2013 and 2014. Day-of-sample fixed effects (FEs), city FEs, and interactions between city FEs and HSR connection are included in all regressions. The last row of each panel reports HSR's aggregate mitigation effect, which is a 0.7 percentage-point reduction in traveler's likelihood of experiencing extreme pollution in column (1) of Panel (a) and a 0.6 percentage-point reduction in column (1) of Panel (b). Standard errors for coefficient estimates are clustered at the city level. Standard errors for the aggregate impact are estimated from 100 block bootstrap replications with each home city as a block. *** $p < 0.01$, ** $p < 0.05$, and * $p < 0.10$.

Online Appendix

A Additional Data Description and Evidence

Summary Statistics Table A1 presents summary statistics for key variables used in this analysis. There are a total of 330,819 city-day observations for $PM_{2.5}$ readings and 466,551 city-day observations for temperature from 2013 to 2016. Some cities did not have $PM_{2.5}$ monitoring stations in the beginning of our sample, which explains $PM_{2.5}$'s lower number of observations. The average daily $PM_{2.5}$ is 52.19 $\mu g/m^3$. This is considerably higher than U.S.'s daily standard of 35.4 $\mu g/m^3$. About 19% of the city-days also exceeded China's daily standard of 75 $\mu g/m^3$ (which became effective in 2016).

$PM_{2.5}$ varies considerably in our sample period, with a standard deviation of 44.51 $\mu g/m^3$ and an inter-quartile range of 40.3 $\mu g/m^3$. The 90th, 95th, and 99th percentiles are 100.8, 131.8, and 219.8 $\mu g/m^3$, respectively. About 80% of the variation comes from day-to-day changes within a city, while the remaining 20% arises from differences across cities (within vs. between variation in a panel setting). The average temperature is 57.96 $^\circ F$, also with a sizeable standard derivation (20.2 $^\circ F$) and inter-quartile range (29.3 $^\circ F$). Similar to pollution, within-city variation accounts for a lion's share (three-quarters) of total variation in temperature. The cutoff for extreme heat in our baseline analysis is 90°F, the 99th percentile of the temperature distribution. The 95th percentile is $83^\circ F = 26^\circ C$, which appears as a very mild cutoff for hot days. The cutoff for extreme cold is 30°F. Using 30°F and 90°F as cutoffs, extreme temperature occurs in around 10% of city-days.

Additional Descriptive Evidence We present additional descriptive evidence on patterns of adaptation to environmental extremes and the role of transportation infrastructure in facilitating such adaptation. Figure A3 is analogous to Figure 1 and presents descriptive evidence on the benefit of improved transportation networks in mitigating households' exposure to extreme temperature. The top panel plots the temperature level experienced by travelers against temperature levels at their home cities. The colored lines represent the local polynomial smoothed averages of the raw data for city-days with HSR connections (blue) and city-days without HSR (red), respectively. The bottom panel presents the empirical temperature distribution for city-days with HSR (blue) and city-days without HSR (red).

Travelers with HSR connections experience warmer temperatures during cold seasons (temperature below 37°F) at home and cooler temperatures during mild and hot seasons (temperature above 37°F). These differences can reach 5 degrees and are statistically significant throughout most of the

distribution, except in the tails when estimates are noisier.[13] The bottom panel shows that the home city's temperature is slightly higher for city-days with HSR access. This is largely due to cross-sectional variation, as cities with HSR are more likely to be found in the warmer south. Figure A3 complements Figure 1 in the main text and provides descriptive evidence on the benefit of improved transportation networks in mitigating households' exposure to adverse environmental conditions.

Figure A5 further maps the geographical distribution of HSR's impact in reducing pollution exposure across cities during each city's 50 most polluted days between 2014 - 2016. The outcome variable is the difference in $\mu g/m^3$ between the pollution level at the home city and travelers' actual exposure. Hence the figure illustrates travelers' benefit of leaving their home city during their home city's 50 most polluted days between 2014 - 2016. A larger positive number denotes a higher benefit. Cities outlined by thick black borders were connected to the HSR network by 2013. We use the most polluted days between 2014-2016 instead of 2013-2016 since some cities did not have HSR connections during the winter of 2013 when several episodes of extreme pollution occurred.

Cities that experience larger reductions in travelers' pollution exposure, on days of intense home exposure, are shown in darker green. It is evident from the map that cities with HSR connections are more likely to exhibit larger reductions relative to their neighbors without such connections. Cities that reap the greatest benefit in pollution reduction tend to be located in Northern China, which has experienced the country's worst pollution over the past decade, especially in winter months.

Figure A6 presents travelers' benefits in terms of temperature exposure in each city's 50 hottest (left panel) and 50 coldest days (right panel) during 2014 - 2016. Travelers' benefit is measured by the difference between their actual exposure and the temperature at the home city. Darker green colors represent travelers experiencing cooler temperatures during hottest days (left panel) and warmer temperatures during coldest days (right panel). Cities in Southeastern China with HSR access display the largest benefits during the hottest days, as the majority of these cities falls into the humid subtropical climate category and are vulnerable to heat waves. Similarly, cities in Northeastern China with HSR access benefit more on the coldest days, when the temperature falls below zero. These trips are facilitated by several north-south HSR lines that travel across a wide temperature range (e.g. the Beijing - Wuhan line). The contrast between cities on and off the HSR lines reflects the mitigating effect of HSR connections, except for southeastern cities in cold days when these cities are much warmer than the rest of the country.

Table A2 illustrates travel patterns by destination cities' temperature, analogous to Table 1. Since extreme temperature includes both cold and hot days, we divide the temperature distribution into ten bins (decile), five bins for temperatures below 61 $^\circ F$ (the median) and five bins for temperatures

[13] The standard errors are calculated using the Epanechnikov kernel and optimal bandwidth in STATA.

above 61 $^{\circ}F$. Each row of the table reports the fraction of travelers visiting each of the ten temperature bins, conditioning on the decile of home temperature. The last two columns report the average temperature experienced by travelers and that at their home city. Panels (a) and (b) present the statistics for travelers' from non-HSR cities and those from HSR cities, respectively, and Panel (c) reports their difference. For example, when the home city's temperature is in the coldest decile, travelers with HSR access are 8.6 percentage points more likely to visit warmer destinations than travelers without HSR access. Similarly, when the home city's temperature is in the highest decile, travelers with HSR access are 7.7 percentage points more likely to visit cooler destinations than travelers without HSR access. Table A2 complements Table 1 in the main text and provides additional descriptive evidence on the benefit of improved transportation networks.

B Appendix Figures and Tables

Figure A1: Expansion of the HSR network

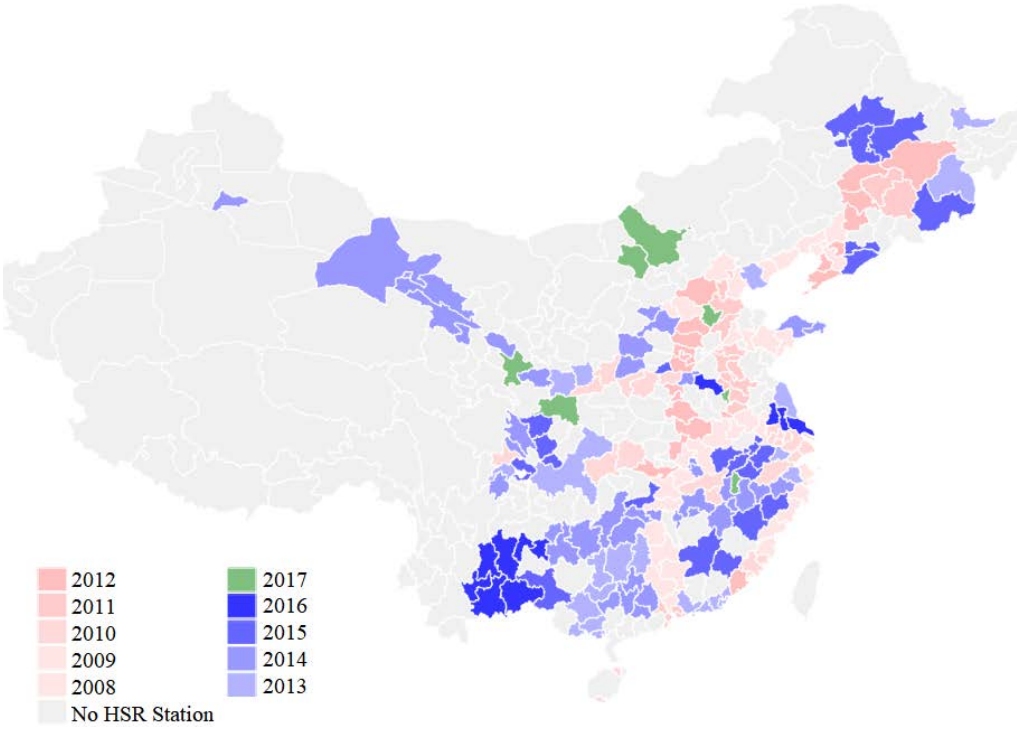

Year	In 2010	'11	'12	'13	'14	'15	'16	'17
HSR network								
# Cities Added	55	16	21	23	40	25	11	7
# Cities in Network	55	71	92	115	155	180	191	198
# City-pairs Connected	196	524	2710	4234	6042	6884	-	-

Notes: This map depicts the rollout of the HSR network from 2008 to 2017. Different colors represent the year when a city is first connected to the HSR network.

Figure A2: Validation using Baidu Migration Data

(a) Population Outflow

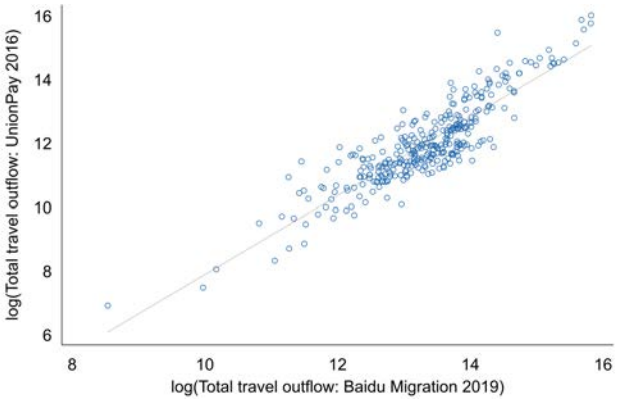

(b) Population Inflow

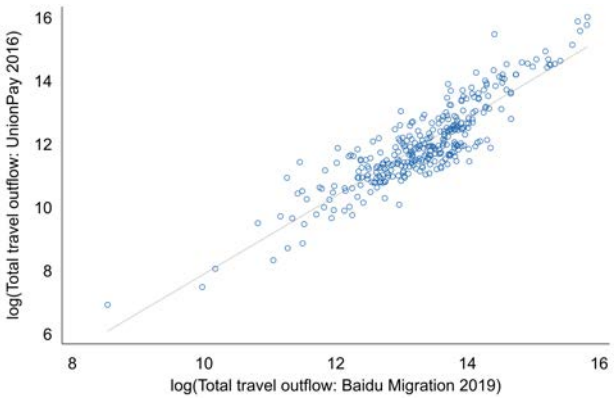

(c) Gravity Equation Estimates

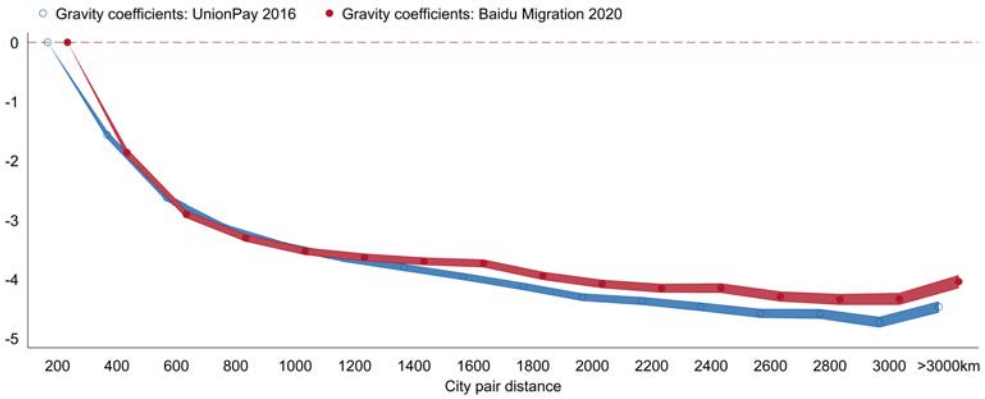

Notes: Panel (a) plots the total number of outbound trips (in logarithm) originating from each city using UnionPay data on the y-axis against that using the Baidu Migration index on the x-axis. Panel (b) plots the total number of arriving trips (in logarithm) from each city using UnionPay data on the y-axis against that using the Baidu Migration index on the x-axis. Each dot represent a city. Panel (c) plots the estimates of β from the gravity Equation below based on city-pair bilateral trips from UnionPay data and the Baidu Migration Index, respectively.

$$ln(n_{ij}) = \sum \beta_k I_k + \alpha_i + \gamma_j + \varepsilon_{ij},$$

where n_{ij} is the aggregate trips between i and j in 2016 for the Unionpay data and in 2019 for Baidu data (only available from 2019). I_k stand for fifteen 200km interval distance bands (0-200km is chosen as the base group). There are 328 observations. The R^2 from both regressions is 0.791, suggesting a high correlation between these two measures.

Figure A3: Travelers' exposure to temperature vs. home exposure

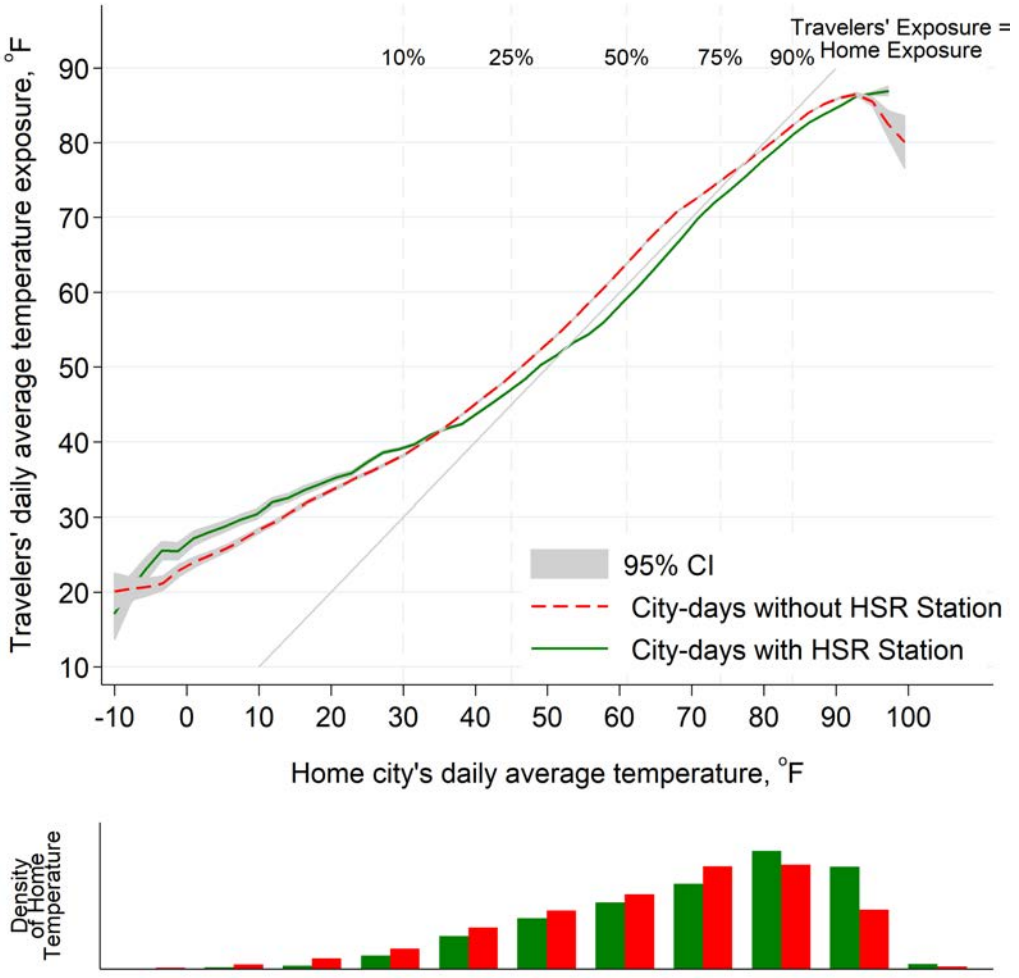

Notes: The top figure plots temperature level experienced by travelers (y-axis) against temperature level at home city (x-axis), separately for city-days with access to HSR (green line) and city-days without access to HSR (red dash line). Both lines are local polynomial regressions weighted by Epanechnikov kernel with optimal bandwidth. The gray area is the 95% confidence interval. The bottom figure displays the distribution of daily temperature at home cities, separately for city-days with access to HSR (green bars) and city-days without access to HSR (red bars). Gray vertical lines mark the 10^{th}, 25^{th}, 50^{th}, 75^{th}, and 90^{th} percentiles of the temperature distribution.

Figure A4: Trip distance for city-days during clean and polluted days

(a) Trip distances during clean days

(b) Trip distances during polluted days

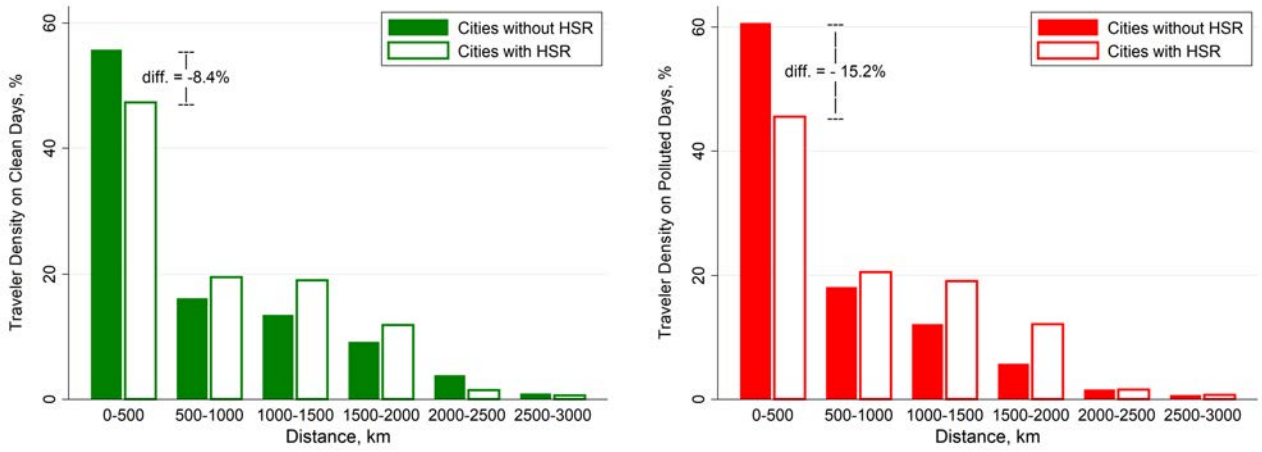

(c) Difference in trip distances

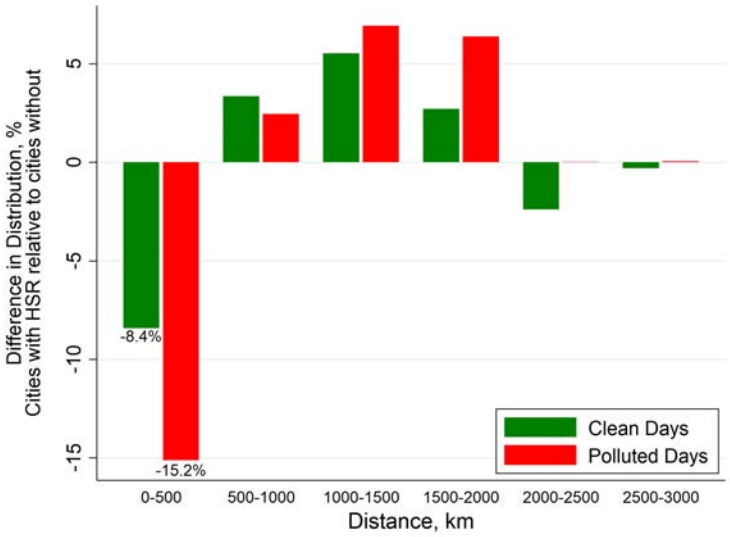

Notes: Panels (a)-(b): histograms for trip distances for cities without or with HSR access during clean and polluted ($PM_{2.5} > 100\mu g/m^3$) days. Panel (c) plots differences in traveler density between cities with HSR access and cities without, on clean days (green bars) and polluted days (red bars). Travelers from cities with HSR access are more likely to visit distant destinations and especially so when home cities experience extreme pollution.

Figure A5: The HSR network and exposure to pollution extremes

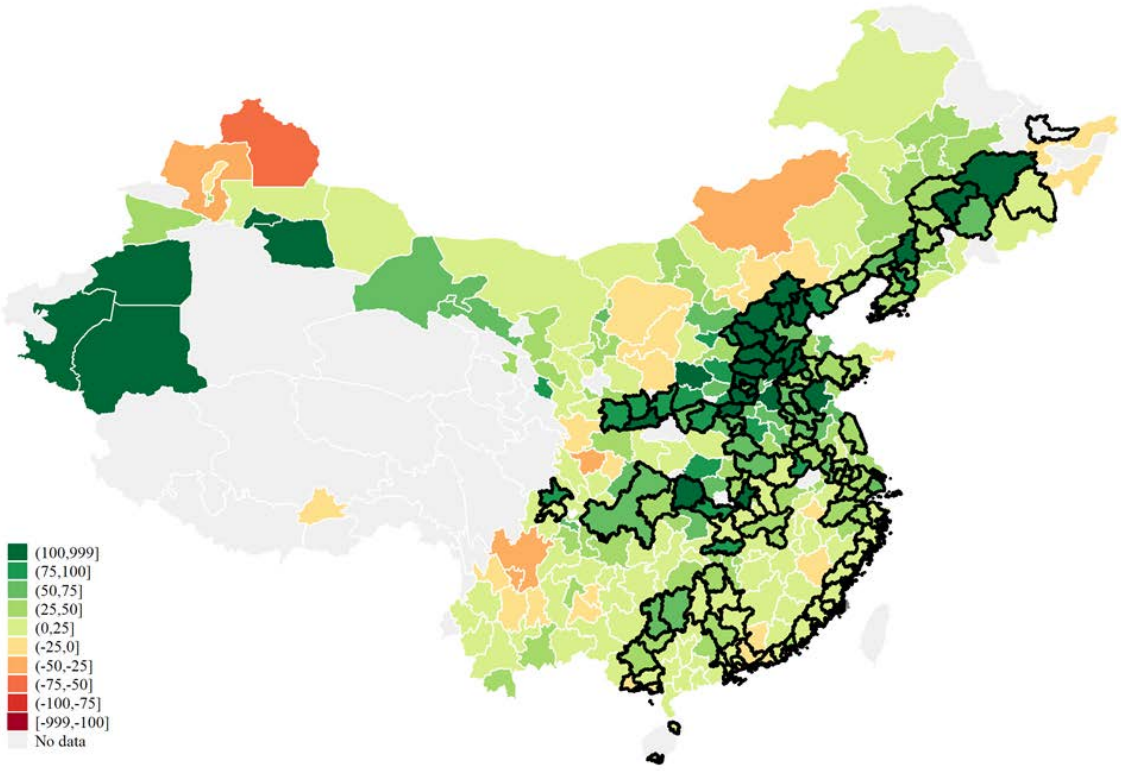

Notes: This figure plots the difference in pollution levels ($\mu g/m^3$) between home and travel destinations, weighted by the number of outbound travelers, during each city's 50 most polluted days between 2014 - 2016. Green colors indicate travelers experiencing less pollution in their destinations than at home; red colors denote travelers experiencing more pollution in their destinations than at home. Cities outlined in black are connected to the HSR network by 2013. Cities with the fewest 10% travelers are not color-coded as traveler exposure in these cities is more prone to measurement error.

Figure A6: The HSR network and exposure to temperature extremes

(a) 50 Hottest Days

(b) 50 Coldest Days

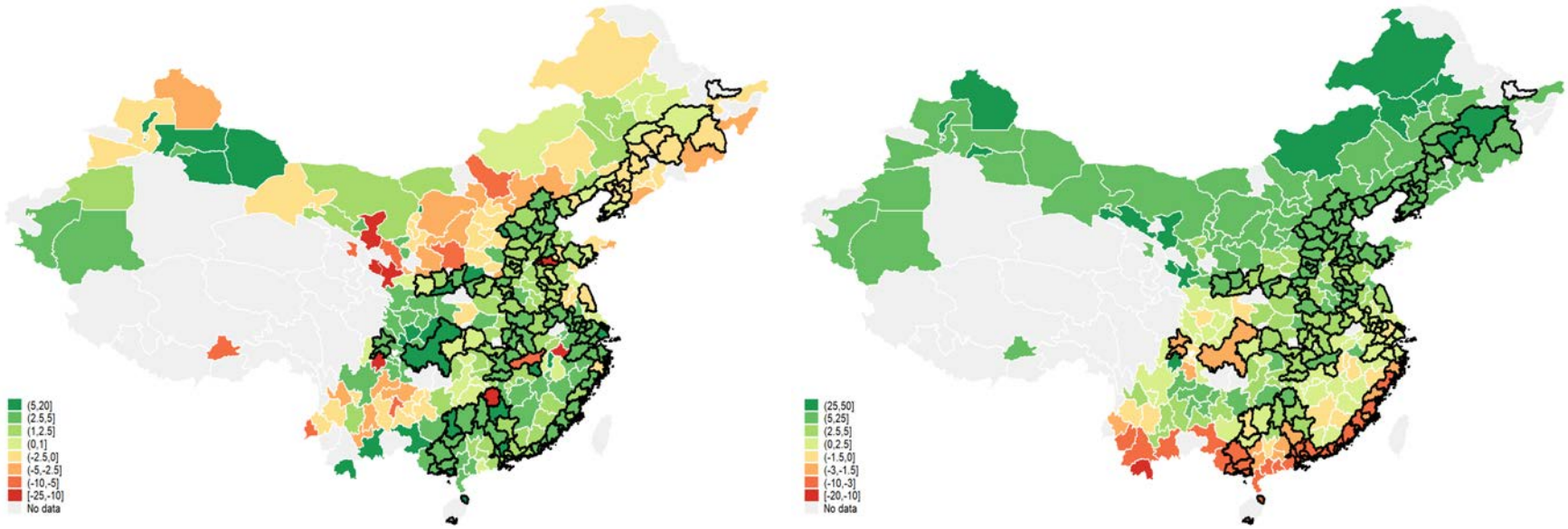

Notes: This figure plots the difference in temperature levels between home and travel destinations, weighted by the number of outbound travelers, during each city's 50 hottest days (left panel) and 50 coldest days (right panel) between 2014 - 2016. The difference is measured as home temperature minus weighted temperature at destinations for the hottest days (left panel) and reversely as weighted temperature at destinations minus home temperature for the coldest days (right figure). Green colors indicate travelers experiencing milder temperatures than at home; red colors denote travelers experiencing more extreme temperatures than at home. Cities with black borders are connected to the HSR network by 2013. The contrast between cities on and off the HSR lines reflects the mitigating effect of HSR connections, except for southeastern cities in cold days when these cities are much warmer than the rest of the country. Cities with the fewest 10% travelers are not color-coded as traveler exposure in these cities is more prone to measurement error.

Figure A7: Event study: HSR opening and outbound travel

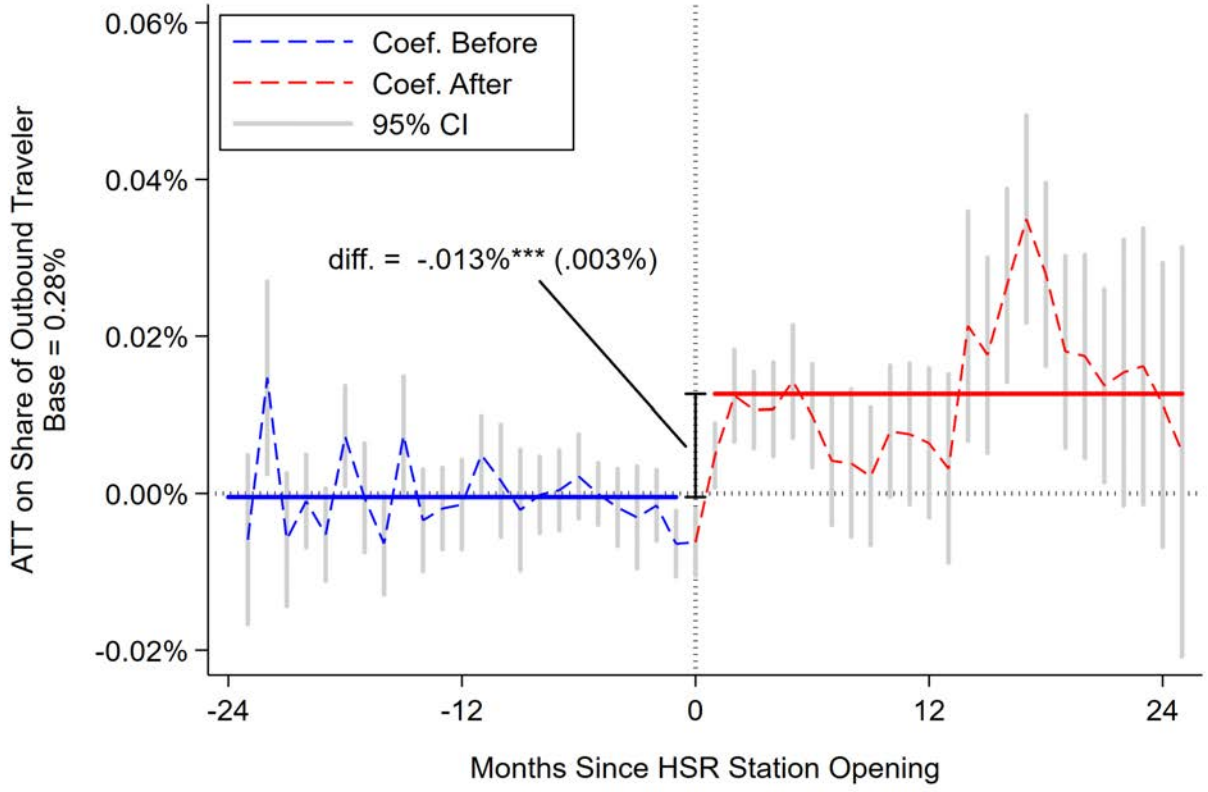

Notes: This graph shows the event study coefficients of HSR opening on a city's share of outbound traveler relative to its population, based on the staggered DID estimation procedure proposed in Callaway and Sant'Anna (2021) and Sant'Anna and Zhao (2020). We restrict the sample to cities with HSR connection by the end of our sample period, and exploits the comparision between early-connected cities and yet to be connected ones. The average treatment effect of HSR opening on the outcome variable is 0.013 percentage point, a 5% increase from the base of 0.28 percentage point.

Table A1: Summary statistics

	Mean	Std. Dev.	Min	Max	Number of Obs.
$PM_{2.5}$, $\mu g/m^3$	52.19	44.51	0	1782.98	330,819
$\mathbb{1}\{PM_{2.5}>100\}$	0.10	0.30	0	1	330,819
Temperature, °F	57.96	20.22	-37.5	104.7	466,551
$\mathbb{1}\{$Temperature$< 30°$F or $> 90°$F$\}$	0.10	0.30	0	1	466,551
Number of travelers	189.65	500.12	1	15,013	486,209
HSR	0.42	0.49	0	1	486,209

Notes: Variable $\mathbb{1}\{PM_{2.5} > 100\}$ takes value 1 if a city's daily average $PM_{2.5}$ concentration is greater than 100 $\mu g/m^3$ and 0 otherwise. Variable $\mathbb{1}\{$Temperature$< 30°F$ or $> 90°F\}$ takes value 1 if a city's daily average tempearture is lower than $30°F$ or higher than $90°F$ and 0 otherwise. Variable HSR takes value 1 if a city has an HSR station in operation on a given day and takes value 0 otherwise.

Table A2: Travelers' travel patterns and temperature exposure

(a) For travelers from city-days with HSR

		Flow share by temperature decile at destination										Average temperature (°F) at	
		Cold 1	2	3	4	5	6	7	8	9	Warm 10	Home	Dest.
Home in	Cold 1	40.6%	24.0%	11.9%	7.5%	7.8%	4.3%	2.4%	1.0%	0.4%	0.0%	21.8	35.8
	2	14.3%	42.5%	16.6%	9.7%	7.8%	4.5%	2.6%	1.2%	0.6%	0.0%	36.0	41.7
	3	7.0%	18.8%	37.6%	15.2%	9.2%	5.4%	3.3%	2.0%	1.2%	0.2%	44.8	46.9
	4	4.0%	10.8%	16.0%	35.2%	16.0%	7.3%	4.7%	3.0%	2.3%	0.6%	52.1	52.2
	5	3.3%	6.9%	8.5%	16.4%	35.6%	13.7%	6.3%	4.6%	3.4%	1.2%	58.6	56.9
	6	1.8%	4.1%	5.3%	7.6%	16.5%	33.1%	15.0%	7.8%	5.8%	3.0%	64.4	62.5
	7	0.8%	1.9%	2.7%	4.5%	7.3%	15.2%	33.1%	17.9%	10.1%	6.6%	69.4	68.2
	8	0.3%	0.8%	1.6%	2.5%	4.8%	7.2%	16.1%	34.6%	19.8%	12.4%	74.1	72.8
	9	0.1%	0.3%	0.7%	1.6%	2.8%	4.3%	7.9%	17.4%	40.7%	24.2%	79.0	76.8
	Warm 10	0.0%	0.0%	0.1%	0.4%	0.8%	2.0%	4.2%	9.1%	20.5%	62.9%	85.1	81.8

(b) For travelers from city-days without HSR

		Flow share by temperature decile at destination										Average temperature (°F) at	
		Cold 1	2	3	4	5	6	7	8	9	Warm 10	Home	Dest.
Home in	Cold 1	49.2%	22.0%	9.6%	6.7%	5.9%	3.4%	2.0%	0.9%	0.3%	0.0%	18.9	32.6
	2	10.9%	45.6%	19.8%	8.8%	6.4%	3.7%	2.3%	1.3%	0.9%	0.2%	35.9	41.9
	3	3.9%	13.8%	40.2%	20.0%	9.6%	5.2%	3.2%	2.1%	1.4%	0.5%	44.8	48.6
	4	2.2%	6.0%	12.9%	37.4%	19.8%	8.7%	5.3%	3.8%	2.7%	1.2%	51.9	54.8
	5	0.9%	2.5%	4.6%	13.4%	36.0%	18.4%	9.1%	6.6%	5.4%	3.1%	58.6	61.2
	6	0.4%	1.1%	1.9%	4.3%	13.5%	31.2%	19.3%	11.2%	9.2%	7.9%	64.4	67.3
	7	0.2%	0.5%	0.9%	1.9%	4.6%	13.5%	31.7%	20.9%	13.1%	12.6%	69.3	71.7
	8	0.1%	0.2%	0.5%	1.0%	2.4%	5.2%	15.0%	35.6%	24.2%	15.9%	74.0	75.0
	9	0.0%	0.1%	0.3%	0.6%	1.4%	2.5%	5.8%	16.0%	43.3%	29.9%	78.8	78.4
	Warm 10	0.0%	0.0%	0.0%	0.2%	0.5%	1.3%	2.8%	6.0%	18.8%	70.5%	85.0	83.0

(c) Difference between Panel (a) and Panel (b)

		Flow share by temperature decile at destination										Average temperature (°F) at	
		Cold 1	2	3	4	5	6	7	8	9	Warm 10	Home	Dest.
Home in	Cold 1	-8.6%	2.1%	2.3%	0.9%	1.9%	0.9%	0.3%	0.2%	0.0%	0.0%	2.9	3.2
	2	3.4%	-3.1%	-3.1%	0.9%	1.4%	0.8%	0.2%	-0.1%	-0.3%	-0.1%	0.1	-0.2
	3	3.1%	5.0%	-2.6%	-4.8%	-0.3%	0.3%	0.1%	-0.1%	-0.3%	-0.3%	0.0	-1.7
	4	1.9%	4.7%	3.1%	-2.1%	-3.8%	-1.4%	-0.6%	-0.8%	-0.4%	-0.6%	0.1	-2.6
	5	2.4%	4.4%	3.9%	3.0%	-0.4%	-4.7%	-2.9%	-1.9%	-2.0%	-1.8%	0.0	-4.3
	6	1.4%	2.9%	3.3%	3.3%	3.0%	1.8%	-4.3%	-3.4%	-3.4%	-4.9%	0.0	-4.7
	7	0.6%	1.4%	1.9%	2.5%	2.7%	1.6%	1.4%	-3.0%	-3.0%	-6.1%	0.1	-3.5
	8	0.2%	0.6%	1.1%	1.6%	2.4%	2.0%	1.1%	-1.0%	-4.4%	-3.5%	0.1	-2.2
	9	0.0%	0.2%	0.4%	1.0%	1.4%	1.8%	2.0%	1.5%	-2.6%	-5.7%	0.1	-1.6
	Warm 10	0.0%	0.0%	0.0%	0.2%	0.4%	0.8%	1.5%	3.1%	1.6%	-7.7%	0.1	-1.2

Notes: This table complements Figure A3 and illustrates that travelers from cities with HSR are more likely to go to cities with milder temperature levels, compared to travelers from cities without HSR. Panel (a) refers to travelers from city-days with HSR, panel (b) refers to travelers from city-days without HSR, and panel (c) presents the difference between the two. Positive (negative) values are colored in different shades of green (red) according to the numerical magnitude. In panel (a) and (b), each row represents the shares of travelers to destination cities with different temperature decile, conditioning on home-city-day's temperature decile. The decile cutoffs for daily temperature are 30, 41, 49, 55, 61, 67, 71, 76, and 82 °F.

Table A3: Travelers' exposure to environmental extremes with alternative exposure measures

	(1)	(2)	(3)	(4)	(5)	(6)
	Continuous measures of exposure		Alternative cutoffs for extremes			
	$PM_{2.5}$	$\lvert T - 70°F \rvert$	$PM_{2.5} > 120$	$PM_{2.5} > 150$	$T < 25°F$ or $T > 95°F$	$T < 35°F$ or $T > 85°F$
Panel (a) : Discrete measure of connectivity						
$Expo_{it}$	0.34***	0.45***	0.28***	0.27***	0.39***	0.41***
	(0.02)	(0.02)	(0.02)	(0.02)	(0.03)	(0.02)
$Expo_{it} \times HSR_{it}$	-0.06*	-0.04*	-0.05**	-0.04	-0.09**	-0.09***
	(0.03)	(0.02)	(0.02)	(0.02)	(0.04)	(0.02)
N	330,801	466,257	330,801	330,801	466,257	466,257
R^2	0.88	0.95	0.76	0.72	0.77	0.81
Panel (b) : Continuous measure of connectivity						
$Expo_{it}$	0.25***	0.40***	0.19***	0.18***	0.32***	0.33***
	(0.02)	(0.02)	(0.01)	(0.02)	(0.02)	(0.01)
$Expo_{it} \times HSR^{C}_{it}$	-0.04***	-0.03***	-0.04***	-0.04***	-0.07***	-0.06***
	(0.02)	(0.01)	(0.01)	(0.02)	(0.01)	(0.01)
N	330,801	466,257	330,801	330,801	466,257	466,257
R^2	0.88	0.96	0.76	0.72	0.79	0.83

Notes: This table examines robustness to alternative measures of exposure to pollution and temperature, as well as different cutoffs for environmental extremes. The dependent variable is the likelihood that travelers experience environmental extremes defined in Eq. (2). $PM_{2.5}$ and T denote the daily average $PM_{2.5}$ concentration and temperature level, respectively. The column heading denotes the $Expo_{it}$ measure used in the regression. HSR_{it} and HSR^{C}_{it} denote the discrete and continuous HSR connectivity measures, respectively. All regressions are weighted by number of outbound travelers from city i on day t. Day-of-sample fixed effects, city fixed effects and interactions between city fixed effects and HSR are included. Standard errors are clustered at the city level. *** $p < 0.01$, ** $p < 0.05$, and * $p < 0.10$.

Table A4: Travelers' exposure to environmental extremes using sub-samples

	(1)	(2)	(3)	(4)	(5)	(6)
	Excluding 5% days with most/least travels		Excluding 10% days with most/least travels		Cities in top 3 tiers	
	$PM_{2.5} > 100$	$T < 30°F$ or $T > 90°F$	$PM_{2.5} > 100$	$T < 30°F$ or $T > 90°F$	$PM_{2.5} > 100$	$T < 30°F$ or $T > 90°F$
Panel (a): Discrete measure of connectivity						
$\mathbb{1}\{\text{home extreme}\}$	0.27***	0.40***	0.27***	0.39***	0.27***	0.42***
	(0.01)	(0.03)	(0.01)	(0.03)	(0.02)	(0.04)
$\mathbb{1}\{\text{home extreme}\} \times HSR_{it}$	-0.05***	-0.12***	-0.05**	-0.12***	-0.07***	-0.10***
	(0.02)	(0.03)	(0.02)	(0.03)	(0.02)	(0.04)
N	330,029	423,888	273,539	378,911	144,369	165,535
R^2	0.79	0.79	0.78	0.79	0.82	0.81
Panel (b) : Continuous measure of connectivity						
$\mathbb{1}\{\text{home extreme}\}$	0.19***	0.31***	0.19***	0.31***	0.18***	0.31***
	(0.01)	(0.01)	(0.01)	(0.01)	(0.01)	(0.01)
$\mathbb{1}\{\text{home extreme}\} \times HSR^C_{it}$	-0.04***	-0.07***	-0.04***	-0.07***	-0.04***	-0.07***
	(0.01)	(0.01)	(0.01)	(0.01)	(0.01)	(0.01)
N	301,714	423,888	272,364	378,912	144,369	165,535
R^2	0.79	0.81	0.79	0.81	0.83	0.83

Notes: This table examines robustness using sub-samples. Columns (1) and (2) exclude each city's 5% of days with the most card transactions and 5% of days with the least card transactions. Columns (3) and (4) exclude 10% of days with the most and 10% of days with the least transactions. Columns (5) and (6) only keep the large cities defined in the top three tiers. The dependent variable is the likelihood that travelers experience environmental extremes defined in Eq. (2). $PM_{2.5}$ and T denote the daily average $PM_{2.5}$ concentration and temperature level, respectively. $\mathbb{1}\{\text{home extreme}\}$ is an indicator for $PM_{2.5} > 100\mu g/m^3$ in odd columns and daily temperature $< 30°F$ or $> 90°F$ in even columns. HSR_{it} and HSR^C_{it} denote the discrete and continuous HSR connectivity measures, respectively. All regressions are weighted by number of outbound travelers from city i on day t. Day-of-sample fixed effects, city fixed effects and interactions between city fixed effects and HSR are included. Standard errors are clustered at the city level. *** $p < 0.01$, ** $p < 0.05$, and * $p < 0.10$.

Table A5: Travelers' exposure to extreme pollution using leads and lags

	(1)	(2)
	Following Week	Preceding Week
Panel (a): Discrete measure of connectivity		
% of extreme days in home city	0.21***	0.22***
	(0.01)	(0.01)
% of extreme days $\times HSR_{it}$	-0.04***	-0.04***
	(0.01)	(0.01)
N	325,255	325,000
R^2	0.75	0.75
Panel (b): Continuous measure of connectivity		
% of extreme days in home city	0.14***	0.15***
	(0.01)	(0.01)
% of extreme days $\times HSR^C_{it}$	-0.02***	-0.02***
	(0.01)	(0.01)
N	323,807	323,554
R^2	0.75	0.75

Notes: This table examines the effect of HSR using the fraction of days when home experiences extreme pollution in the following or preceding week. The dependent variable is the likelihood that travelers experience environmental extremes defined in Eq. (2). Variable '% of extreme days in home city' is the fraction of days with extreme pollution in the following or preceding week. HSR_{it} and HSR^C_{it} denote the discrete and continuous HSR connectivity measures, respectively. All regressions are weighted by number of outbound travelers from city i on day t. Day-of-sample fixed effects, city fixed effects and interactions between city fixed effects and HSR are included. Standard errors are clustered at the city level. *** $p < 0.01$, ** $p < 0.05$, and * $p < 0.10$.

Table A6: Travelers' exposure to extreme pollution: channels of impacts

Panel (a) : Changes in Travel Distance		
	Hypothetical Travelers' Exposure	
	PM$>$ 100	$T < 30°$F or $T > 90°$F
$\mathbb{1}\{$home extreme$\}$	0.11***	0.21***
	(0.003)	(0.002)
$\mathbb{1}\{$home extreme$\} \times HSR_{it}$	-0.02***	-0.06***
	(0.002)	(0.002)
N	330,801	466,257
HSR's overall impact	-0.003	-0.003

Panel (b) : Longer Horizon Adaptation		
	Hypothetical Travelers' Exposure	
	PM$>$ 100	$T < 30°$F or $T > 90°$F
$\mathbb{1}\{$home extreme$\}$	0.30***	0.49***
	(0.01)	(0.02)
$\mathbb{1}\{$home extreme$\} \times HSR_{it}$	-0.02	-0.07**
	(0.01)	(0.03)
N	330,801	466,257
R^2	0.66	0.74
HSR's overall impact	-0.005	-0.005

Notes: The dependent variable of Panel (a) is hypothetical travelers' exposure that is constructed by replacing destination cities' environmental conditions with the concurrent conditions in cities of a similar distance to the origin, $TravExpo^1_{it} = \sum_{j \neq i} \widehat{Expo_{jt}} \cdot \frac{N_{ijt}}{\sum_{k \neq i} N_{ikt}}$, where $\widehat{Expo_{jt}}$ is the pollution level of a randomly-chosen city that is similarly distant from the original city as city j. $\mathbb{1}\{$home extreme$\}$ is an indicator variable of extreme conditions. Day-of-sample fixed effects, city fixed effects, and interactions between city fixed effects and HSR dummy are included in both regressions. The last row reports HSR's aggregate effect holding trip distance constant, which is a 0.3 percentage-point reduction in traveler's likelihood of experiencing extreme pollution as well as a 0.3 percentage-point reduction in exposure to extreme temperature.

The dependent variable of Panel (b) is hypothetical travelers' exposure that is constructed using the average traveler flow from the origin city before and after HSR: $TravExpo^2_{it} = \sum_{j \neq i} Expo_{jt} \cdot \frac{N^{\text{No HSR}}_{ij}}{\sum_{k \neq i} N^{NoHSR}_{ik}} \cdot \mathbb{1}\{t \text{ before HSR}\} + \sum_{j \neq i} Expo_{jt} \cdot \frac{N^{\text{HSR}}_{ij}}{\sum_{k \neq i} N^{HSR}_{ik}} \cdot \mathbb{1}\{t \text{ post HSR}\}$, where $N^{\text{No HSR}}_{ij}$ is the total number of travelers from city i to city j prior to the HSR access and N^{HSR}_{ij} is the total number of travelers from city i to city j post the HSR access. The last row reports HSR's aggregate mitigation effect in the absence of day-to-day avoidance responses, which is a 0.5 percentage-point reduction in traveler's likelihood of experiencing extreme pollution as well as a 0.5 percentage-point reduction in exposure to extreme temperature. Standard errors are clustered at the city level. *** $p < 0.01$, ** $p < 0.05$, and * $p < 0.10$.

Table A7: Number of outbound travelers in response to extreme pollution at home (the extensive margin)

Dep. var.: number of outbound travelers	(1)	(2)	(3)	(4)	(5)
		Pollution Extremes		Temperature Extremes	
		Current Day	Avg. exposure ($\pm$3 days)	Current-day	Avg. exposure ($\pm$3 days)
HSR_{it}	0.049	0.044	0.041	0.054	0.054
	(0.051)	(0.056)	(0.057)	(0.052)	(0.052)
$\mathbb{1}\{\text{home extreme}\}$		-0.010	-0.028	-0.032***	-0.058***
		(0.013)	(0.036)	(0.0093)	(0.013)
$\mathbb{1}\{\text{home extreme}\} \times HSR_{it}$		0.019**	0.042**	0.010	0.0036
		(0.0085)	(0.019)	(0.0068)	(0.0095)
N	486,209	330,819	325,548	466,551	454,008

Notes: This table examines the extensive margin, i.e. the number of outbound travelers in city i at time t when city i experiences extreme conditions. Coefficients are estimated using Poisson pseudo maximum likelihood (PPML) regression and can be interpreted as semi-elasiticities. $\mathbb{1}\{\text{home extreme}\}$ is an indicator for $PM_{2.5} > 100\mu g/m^3$ in Columns 2 and 3 and daily temperature $< 30°$F or $> 90°$F in Columns 4 and 5. All regressions are weighted by number of outbound travelers from city i on day t. Day-of-sample fixed effects and city fixed effects are included. Standard errors are clustered at the city level. *** $p < 0.01$, ** $p < 0.05$, and * $p < 0.10$.